Research Report
KTC 94-16

Stress Measurements on the I 65 Bridge over the Ohio River at Louisville

by

Theodore Hopwood, II
Transportation Research Engineer
and

Christopher M. Oberst
Transportation Research Technologist

Kentucky Transportation Center
College of Engineering
University of Kentucky
Lexington, Kentucky

in cooperation with
Transportation Cabinet
Commonwealth of Kentucky

and

Federal Highway Administration
U.S. Department of Transportation

July 1994

TABLE OF CONTENTS

EXECUTIVE SUMMARY

Kentucky Transportation Center personnel conducted measurements of live stresses on structural members of the I 65 (John F. Kennedy Memorial) Bridge over the Ohio River. That work was performed in conjunction with an extensive flaw evaluation of the bridge by Hazelet & Erdal Consulting Engineers.

The measurements were performed by placing strain gages on the upper chord (an H-beam) and a vertical post and transverse strut that were framed into the upper chord at PP63 on the West truss. Measurements were performed using battery-powered data logging instruments that were capable of unattended strain measurement. The units were used to monitor live stresses induced by routine traffic. Specific tests included short duration time-history measurements on the three structural members, a short duration strain gage rosette measurement on the upper chord and a day-long stress histogram measurement also on the upper chord.

The time-history measurements were intended to measure the magnitude of live stresses in the beams. Multiple gages were installed on opposite faces of the structural members for those tests to gain insight into the nature of forces acting on them. The rosette test was performed to measure the principle stresses acting on the upper chord and, thereby, ascertain the nature of forces acting on the upper chord. The stress histogram measurements were conducted to determine the magnitudes of live stresses and number of stress cycles over an extended period.

The time-history test data revealed low magnitude live stresses at all the test locations. The maximum tensile live stresses measured were: 1) 1,147 psi for the upper chord, 2) 2,230 psi for the vertical post and 3) 580 psi for the transverse strut. The rosette test yielded a maximum principle stress of 1,120 psi. The stress histogram data indicated that the variable-amplitude live stresses acting on the bridge were comparable to a constant-amplitude live stress of 1,660 psi at a rate of 773,864 cycles per year.

Comparisons of stress data taken on the upper chord indicated that is was subject to some non-axial forces. Similar measurements taken on the vertical post indicate that it was subject to transverse forces possibly induced by the strut.

Based upon the low stress magnitudes measured during the tests, it appears that live stresses generated by traffic do not have a significant impact on the structural integrity of the bridge.

INTRODUCTION

Background

Kentucky Transportation Center (KTC) personnel applied strain gages on the I 65 (John F. Kennedy Memorial) Bridge over the Ohio Bridge at Louisville, KY and subsequently performed a series of stress measurements. That work was performed in conjunction with nondestructive inspections and structural and metallurgical analyses supervised by Hazelet & Erdal (H&E) Consulting Engineers Inc. of Louisville for the Kentucky Transportation Cabinet (KyTC). The inspections, testing and analyses were prompted by cracks detected in butt welds on the upper chords of the bridge's truss members. The use of quenched and tempered steel for the upper chord members also concerned KyTC officials since welds incorporating that material may become embrittled due to the presence of hydrogen.

The purpose of the strain-gage tests was to measure the magnitude (and frequency) of live stresses induced by routine traffic in several structural members. KTC personnel were also to analyze the resulting data and determine the structural responses of the selected bridge members to those live loads. Four separate tests were planned to meet those objectives.

Test Descriptions

Test 1 was intended to measure axial live stresses along the upper chord, an H-beam. Strain gages were installed on the upper chord near panel point PP63 on the West truss. At that point, a transverse strut was framed into the upper chord. The strut was unbraced and vibrated when heavy traffic (multiple trucks) passed over the bridge. It was suspected that the vibrations might provide live stresses unanticipated in design that might promote cracking in the butt welds. The gages were aligned with the longitudinal axis of the H-beam.

Both flanges of the upper chord H-beam were strain gaged below the web at diametrically opposite locations on the interior faces of the flanges. The gages were located in the thinner section of the flanges about 2 inches below the web, approximately 7 inches from the transition butt welds.

The variable amplitude live stresses measured by the two gages were to be compared to determine whether they were identical. It was anticipated that those stresses would be identical in magnitude and phase if the upper chord was subjected to axial forces. If that was not the case, it would indicate that the upper chord was being subject to transverse forces provided by the strut.

Test 2 was conducted on a vertical post and on the transverse strut that were framed into the upper chord at PP63. Strain gages were mounted on exterior faces of the inboard and outboard sides of the box member that comprised the vertical post. The gages were positioned at the center of the faces, aligned along the longitudinal axis of the post. They were mounted 4 inches below splice plates that connected the post to the upper chord.

Strain gages were also placed on the exterior faces of the upper and lower flanges of the

strut, a rectangular box member, adjacent to the upper chord. Those gages were aligned along the longitudinal axis of the strut. The upper gage was located at the center of the upper flange approximately 11 inches from a splice plate that connected to the upper chord. The lower gage was located on the center of the lower flange approximately 3 inches from a splice plate also connected to the upper chord. Both gages were located equidistant from the end of the strut.

The objective of the live stress measurements at the vertical post test locations was to determine whether the strut vibration induced significant live stresses in the post. By design, the vertical post was not expected to experience live stresses. Comparison of any live stresses measured by the gages mounted on the vertical post might indicate the manner of force application. If they differed in magnitude or phase, it might indicate that strut vibrations were inducing transverse live stresses in the post.

Live stresses measured on the strut could be used to determine the magnitude of transverse forces exerted by the strut on the upper chord member at the connection. Comparisons of the magnitude and phases of the live stresses measured by the two gages located on the strut might provide insight concerning strut motion. Comparisons of the magnitudes and phases of live stresses in the strut with those in the vertical post and the upper chord might indicate whether strut motion had a significant effect on those members.

Test 3 involved placing a 3-strain gage rectangular rosette on the inner face of the thinner section of the inboard flange of the upper chord H-beam, 1 1/2 inches from the lower edge of the flange and 36 inches from the transition weld.

That test was intended to indicate whether only axial forces were exerted on the upper chord. The rosette was aligned with its center gage oriented along the longitudinal axis of the upper chord. If the upper chord was subjected only to axial forces, the live stresses measured by that gage would correspond to the values of maximum principal stress (within the limits of experimental error).

For tests 1-3, concurrent time-history measurements were to be performed at the test locations. Each of the time-history tests were set to last 30 minutes (1,800 seconds). The SoMat was programmed to digitally sample the analog strain gage data at a rate of 75 Hz. That provided 135,000 data points per test. The resulting data were to be reviewed primarily to determine magnitudes of the greatest live stresses.

Test 4 was intended to quantitatively assess live stresses acting on the upper chord at the transition butt weld in terms of both magnitude and number of cycles accumulated over the test period. The two strain gages employed on the upper chord H-beam flanges for test 1 were also used in this test. The **SoMat** evaluated live stress measurements "on-the-fly" by rainflow counting and stored the data as stress histograms. The resulting stress histograms provided the number of live stress cycles that occurred over the monitoring period in terms of preselected stress-range "bins." Bin intervals used for the test were graduated in 500 psi increments.

To determine the potential for fatigue problems, the derived stress histogram data must

be converted into a constant-amplitude stress range equivalent in impact (damage) to all the variable-amplitude live-load stresses measured. That can be accomplished using the Miner equivalent stress equation:

$$S_{re(Miner)} = (\sum P_i * S_{ri}^3)^{1/3}$$

where

$S_{re(Miner)}$ = the equivalent stress range,

P_i = the proportion of stress cycles for S_{ri}, and

S_{ri} = the preselected stress range or midwidth of the i^{th} interval.

The single-valued stress range, $S_{re(Miner)}$, represents an equivalent constant-amplitude stress for the complete data set that will result in the same amount of fatigue damage when applied in place of the variable-amplitude live stress spectrum given by the stress histogram.

To properly assess the live stresses induced by traffic, the stress range measurement should be taken for a time interval that is representative of long-term service. Usually, monitoring for a week (or more) is desirable. Time constraints in this study limited the monitoring period to 24 hours.

Test Instrumentation

For the strain gage measurements, **SoMat** Model 2000 signal conditioner/data loggers were employed. Those are compact battery-powered units that permit unattended monitoring of strain gages at remote locations. Portability of the **SoMats** allows them to be stored on a large structure near strain gage test sites thereby minimizing signal wire runs. That lowers the systems susceptibility to false data caused by electrical noise.

The **SoMats** are microprocessor-based and can be pre-programmed to perform a variety of data-acquisition routines including time-history and rainflow counting. The units may be: 1) pre-programmed to run a particular test, 2) calibrated to provide strain gage signal conditioning (power and signal measurement) and 3) left unattended to record strain gage data over a pre-selected test interval. Once a test is completed, the data is retained by the units in non-volatile memory. The unit may be accessed at the convenience of the operator who retrieves the data by uploading it from the **SoMat** to a portable PC.

The strain gages used in this study are foil resistance (350-ohm) gages. The gages were bonded to the bridge steel using an isocyanate glue. The gages were wired to the **SoMats** and operated in a three-wire, quarter-bridge configuration. In that mode, the **SoMats** are able to perform auto-calibration using internal wheatstone bridge resistors.

FIELD TESTS

Due to traffic limitations, the various test functions (strain-gage installation, instrument set-up and calibration, test start-up, and data retrieval) needed to be performed at night

when lane closure was permitted and a man-lift was available. H&E personnel desired to obtain stress data during the morning traffic rush hours (between 6:30 to 8:30 am on weekdays). By that time, all personnel working on the bridge the preceding night were required to leave the work site to provide motorists with an unhindered roadway. During weekdays, high traffic volumes would be present on the bridge in the morning rush hours.

Those operational time constraints impacted tests 1-3. A feature of the **SoMats** allowed the units to be programmed to delay recording data for a pre-determined period after calibration and test initialization. For tests 1-3, a **SoMat** recorded data for the preselected test interval (30 minutes) in the time-history mode. Thereafter, it shut down retaining the data in internal memory.

Test 4 did not require the delayed data recording feature. Data acquisition began as soon as the **SoMat** was programmed and calibrated. It terminated at the end of the 24-hour test interval.

Absolute stress values were required for tests 1-3. There was some concern that the temperature of the steel might change in the time interval between test initialization and data acquisition possibly impacting the strain measurements. For those tests, a second **SoMat** was employed with a resistance temperature sensor to measure the temperature of the steel during that time interval to permit thermal correction of the data. Subsequent review of the temperature data revealed that temperature changes during those tests were inconsequential. Test 4 did not require temperature measurements.

All of the tests were performed during week days. Tests 1 and 2 were performed on the morning of April 19 and 21, respectively. Test 3 was performed on the morning of May 18. Test 4 was initiated on the evening of May 18 and was terminated on May 19. During an evening following a test, KTC personnel returned to the test site and uploaded the data to a portable PC. The **SoMats** and their batteries were housed in tool boxes stored in the vertical post at PP63 adjacent to the upper chord throughout the tests.

DATA ANALYSES

Strain Gage Nomenclature

The following identification will be employed for the strain gages:

Test 1

I65121 - The strain gage mounted on the inner face of the outboard flange of the upper chord H-beam.

I65122 - The strain gage mounted on the inner face of the inboard flange of the upper chord H-beam.

Test 2

I65363 - The strain gage mounted on the outboard face of the vertical post box beam.

I65364 - The strain gage mounted on the inboard face of the vertical post box beam.

I65365 - The strain gage mounted on the lower face of the strut box beam.

I65366 - The strain gage mounted on the upper face of the strut box beam.

Test 3

I6571 - A rosette strain gage aligned 45° downward to the longitudinal axis of the upper chord H-beam.

I6572 - A rosette strain gage aligned with the longitudinal axis of the upper chord H-beam.

I6573 - A rosette strain gage aligned 45° upward to the longitudinal axis of the upper chord H-beam.

Test 4

I6581 - The strain gage mounted on the inner face of the outboard flange of the upper chord H-beam (same as I65121).

I6582 - The strain gage mounted on the inner face of the inboard flange of the upper chord H-beam (same as I65122).

Time-History Data

Time-history strain traces for Tests 1-3 are provided in Appendix A. Those data were converted to stresses by multiplying the strain data (in microstrains, where 1 microstrain = $1x10^{-6}$ in./in,) by the modulus of elasticity for steel (29 $x10^{6}$ psi).

Inspection of the time-history data revealed that the at-rest or "zero" position of the strain gage signals for most tests had shifted in the interval between instrument calibration and data recording. Those shifts could not be attributed to temperature changes in the steel during the test period. Inspection of the data indicated the shifts were related to test equipment factors (sensors and instrumentation) rather than to traffic. They may be due to equipment instability during data recording or to internal heating of the strain gages caused by electrical excitation. Since the data did not drift during data acquisition, the shifts were probably caused by strain gage heating during the dormant portion of the tests.

To correct for that error, it was necessary to ascertain the at-rest live stress level of the variable-amplitude test data. That was accomplished either by: 1) inspecting the data and visually determining the at-rest live stress level or 2) averaging all of the data to determine the mean value of the live stress. For each test, the data were adjusted by subtracting or adding either the computed mean value or the visually determined at-rest

live stress offset from each data point. The live stress shift compensation (corrections), the adjusted mean, the adjusted maximum and minimum live stresses, and total live stress ranges for each test were computed (Table 1). Subsequent data analyses used the adjusted live stress values.

A PC data analysis and display program, **DaDisp**, was employed for data correction and other data analyses. That program allowed direct comparison between the data sets by overplotting. Data were plotted on **DaDisp** for visual inspection. Plots of time-history live stresses over the entire test interval were made for each strain gage involved in tests 1-3 (Figures 1-9). Peak maximum tensile stresses were identified and plotted over short time bases to provide better resolution (Figures 10-18). Live stresses of the comparative test sets (I65121 and I65122, I65363 and I65364, and I65365 and I65366) were overplotted for 1) all data and 2) short time intervals (10 to 50 seconds) to display comparative live stress magnitudes and to reveal any relevant phase variations (Figures 19-24).

For test 3, **DaDisp** was used to compute 1) the maximum and minimum principle live stresses, 2) the maximum live shear stress and 3) the angle between the maximum principle live stress and the axis of gage I6572 (aligned with the longitudinal axis of the upper chord H-beam). Stress data from I6572, along with the concurrent data from gages I6571 and I6573, were used in those computations which were based upon a condition of plane stress. The maximum principle live stresses for all data were overplotted with data from I6572 in Figure 25.

Data Validation

The data from tests 1 and 2 (Figures 1-6) exhibited many low-amplitude stress cycles of constant peak values. Close inspection of the data revealed that the stress cycles occurred over variable time intervals. The time-base signal widths of most of the stress cycles were large indicating that they occurred at low frequencies. Both of those factors indicated that the data were probably from valid events.

To ensure that the data were not corrupted by 60 Hz (or higher frequency) electric noise, fast fourier transforms (FFTs) were performed on the data from tests 1 and 2 (Figures 27-32). FFTs are used to extract frequency-domain information from data acquired in the time domain (time-history data). The resulting plots show the relative amounts of energy of specific frequencies that comprise a specific data set. The y-axis of the plots shows the relative energy of the data and the x-axis the frequencies at which those events occur. Large relative energy values usually occur at specific frequencies or frequency bands. They indicate the frequency(s) of measured data such as live stresses that result from dynamic events such as bridge loadings by traffic. The frequencies of most commonly occurring events will provide high energies that exceed the background energies of other less-relevant frequencies that comprise the test spectrum. A sharp peak at a specific frequency that is repeated at integer multiples typically indicates harmonic resonance. The data may be corrupted by electric noise if large relative energies occur at high frequencies.

The limiting frequency for FFTs is equal to one-half the digital sampling rate or, in this

case, 75 Hz/2 = 37.5 Hz. Plots of FFTs produce a mirror image about that frequency and data above 37.5 Hz are ignored.

Data in the frequency bandwidth between 1-15 Hz were of interest since that are considered the normal frequency range for most valid data - data outside that bandwidth is usually considered extraneous. Based upon the data acquisition frequency (75 Hz) and the anticipated frequency of electric noise (60 Hz), the 15 Hz limit also constitutes the upper permissible limit for post-test filtering of the digitized data.

The data were digitally bandpass filtered between 1 Hz and 15 Hz using a butterworths filter. The filtered data were analyzed for frequency content by performing FFTs. The filtered and unfiltered FFTs were compared and no significant differences were observed. That indicates that most of the recorded data are related to valid sources (changes in stress due to live loads).

The constant values of the low-amplitude stress peaks are believed to be due to quantization error. That phenomenon is related to the ability of the **SoMats** to resolve the measured data. Design of the **SoMats** limits their ability to balance properly to a minimum stress range or span of 60,000 psi. As the units digitize data in an 8-bit mode, their theoretical limit of resolution is $\pm$ 234 psi. Inspection of the **SoMat** data revealed a slightly higher limit of resolution (about 300 psi). Data are only recorded in increments of approximately 300 psi and, as a result, all live stresses that occurs within the range of one of those increments will be recorded at equivalent values. Due to the relatively coarse system resolution and low magnitude of most of the live stresses, most of them were recorded as being equivalent.

Rainflow Analyses

The rainflow data obtained in test 4 from strain gages I6581 and I6582 were downloaded to a spreadsheet as stress histograms (Figures 33 and 34). Data considered valid for analysis had bin centering values from 750 to 15,250 psi. Out-of-range data were disregarded. The Miner equivalent stresses were computed from the stress histogram data (Tables 2 and 3).

CONCLUSIONS

Test 1 - The adjusted live stress plots for the two strain gages mounted on the upper chord (I65121 and I65122) indicate that the upper chord H-beam experienced stress reversals due to live loading (Figures 1 and 2). The total range of live stresses for I65121 was slightly greater (by approx. 500 psi) than that for I65122. That is reflected by both the maximum and minimum stresses measured by the two gages. The live stresses measured at the two flanges were of low magnitudes (less than 1,500 psi). Most of the higher magnitude live stress peaks correspond between the two gages as do some lower magnitude live stress peaks (Figures 19 and 20). While the live stress traces are similar, they are not identical. The maximum tensile stresses for the two test locations did not occur concurrently (Figures 10 and 11). The live stress variation between the two flanges of the H-beam may be due to joint effects or, in part, to strain gage mounting errors. It is likely that some forces acting on the upper chord were not axial.

Test 2 - The strain gages (I65363 and I65364) located on the vertical post appeared to have measured more live stress cycles than the gages mounted on the upper chord. Many of the stress cycles measured on the vertical post were of very low values occurring at the **SoMat's** limit of data resolution. A few higher magnitude stresses, both tensile and compressive, were observed at both locations. Most of the low magnitude stresses for the gage mounted on the West face (I65363) were compressive, while those for the strain gage mounted on the East face (I65364) were primarily tensile (Figures 3 and 4). The stress traces appeared to be mirror images (i.e. compression vs tension) that were similar, but not identical (Figures 21 and 22). The opposing stresses indicate that the vertical post was acting in bending with a few reversals. The maximum tensile live stresses for the strain gage sites did not occur concurrently (Figures 12 and 13).

The stress traces for the strain gages mounted on the strut (I65365 and I65366) indicate that both locations primarily experienced tensile live stresses (Figures 5 and 6). A few relatively large compressive live stresses were measured by the lower gage. More tensile and compressive live stress cycles were measured by the upper gage. Typically, low-amplitude live stresses (300 psi or less) were measured at both locations. The maximum tensile live stresses did not occur concurrently (Figures 14 and 15). There was no discernable relationship between live stresses at the two test sites either by phase or magnitude (Figures 23 and 24).

Test 3 - The rectangular strain gage rosette was mounted so that strain gage I6572 was oriented along the longitudinal axis of the upper chord H-beam. If only axial loading occurred on the upper chord, the stress measurements from that gage would equal the computed values for the maximum principle stress. The stress traces for the rosette indicated that the upper and middle gages (I6573 and I6572, respectively) were experiencing stress reversals while the lower gage (I6571) was cycling in tension (Figures 7-9). The maximum tensile stress values for all three strain gages occurred several times throughout the test period, but only once concurrently (Figures 16-18).

Data for the three strain gages were used with **DaDisp** to compute the maximum principle live stress for all 135,000 data points assuming a plane stress state. The resulting values were inspected to determine two data points: 1) at the maximum tensile live stress for the center gage (I6572) and 2) at the highest tensile value for the maximum live principle stress.

The maximum tensile live stress value for I6572, 870 psi, occurred several times during the test including the highest tensile value for maximum live principle stress (Figure 25). At the first maximum value for I6572, the maximum principle stress was 1,027 psi, 9°13' from the alignment of the center gage. The highest tensile value for maximum principle stress was computed to be 1,120 psi. That occurred when all of the strain gages were at their maximum tensile stress values. At that point, the minimum principle stress was 671 psi and the maximum shear stress was 225 psi. The maximum principle stress at that point was computed to act along the center gage. However, that is not possible because the maximum principle stress should equal the stress measured by the center strain gage if their axis were coincident. That result is probably an artifact of quantization error.

The overplot of all live stress data for test 4 reveals that the live stresses measured by I6571 and I6573 commonly differ (Figure 26). That indicates forces acting on the H-beam are not entirely axial supporting the conclusion provided by the test 1 data. Since the live stresses measured by the rosette gage were very small (less than 1,000 psi), the consequences of the non-axial forces are probably insignificant.

FFTs for I65121 and I65122 revealed that the frequency content for most of the data was below 10 Hz (Figures 27 and 28). FFTs for I65363 and I65364 on the vertical post indicated a resonant response at 4 Hz and multiples thereof up to about 20 Hz (Figures 29 and 30). It is interesting to note that a 4-Hz peak was also observed in the FFTs for I65365 and I65366 on the transverse strut (Figures 31 and 32). However, resonant frequencies were not observed. The 4 Hz peaks in both the strut and the vertical post reveal that there may be some physical interaction between them. However, the live stresses measured at those locations indicate that interaction is insignificant.

Test 4 - Stress histogram data obtained from strain gages I6581 and I6582 indicate substantially greater live stress magnitudes and number of cycles for the inboard flange. That data differed from test 1 that indicated greater magnitude live stresses for the outboard gage. At this time, there is no firm explanation for that discrepancy. Only minimal weather protection was applied to the strain gages and it is possible that moisture may have infiltrated the outboard gage weakening its bond to upper chord.

The equivalent live stress for the outboard gage (803 psi) and the annual accumulated stress cycles (5,840) appear to be low (Table 2). The equivalent live stress for the inboard strain gage (1,660 psi) corresponds with typical values KTC personnel have previously measured on similar structural members of other truss bridges (Table 3). The projected annual accumulated cycles (773,864) also appear reasonable.

That data may be incorporated in a damage tolerance/fracture mechanics framework to ensure structural reliability. To accomplish that, the equivalent live stress is employed in a fatigue crack growth model that will determine the growth rate with increasing crack size and accumulated number of stress applications (cycles). By assuming a lower bound for the initial crack size, an upper bound for the crack size at failure and the annual accumulation of cyclic stresses, safe inspection intervals may be estimated for various nondestructive evaluation (NDE) methods. That will assure that NDE methods applied will provide a known period of reliability assurance when no cracks are detected.

All of the strain gage tests measured low magnitude live stresses in the three bridge members monitored. Analyses indicated the stress cycles were occurring at frequencies anticipated for normal bridge loading and were not corrupted by electronic noise. Since most of the live stresses measured were of very low magnitude, it is unlikely that they would have an unfavorable impact on structural integrity of the bridge.

TABLES

Table 1. Time-History Live Stress Measurement Data Including Compensation, Adjusted Mean, Adjusted Max., Adjusted Min. and Total Range.

Gage ID	Compen. (psi)	Mean (psi)	Max. (psi)	Min. (psi)	Range (psi)
I65121	+278	-0.01	+1,147	-881	2,028
I65122	+868	-0.01	+868	-584	1,452
I65363	+1,738	-113	+579	-579	1,158
I65364	-870	+84	+2,320	-290	2,610
I65365	0	0	+290	-870	1,160
I65366	-580	-0.01	+580	-290	870
I6571	-4,934	+28	+589	0	589
I6572	-2,609	-205	+870	-870	1,740
I6573	+2,319	-25	+580	-580	1,160

Range (ustrain)	Mid-Stress in Bins, Sri (ksi)	Number of Counts	Proportion of Stress Cycles (Pi)	(Mid-Stress in Bins)^3	Pi*Sri^3
underflow	0.00	0	0.000	0.000	0.000
0.0	0.25	0	0.000	0.016	0.000
16.7	0.75	15	0.938	0.422	0.396
33.3	1.25	1	0.063	1.953	0.122
50.0	1.75	0	0.000	5.359	0.000
66.7	2.25	0	0.000	11.391	0.000
83.3	2.75	0	0.000	20.797	0.000
100.0	3.25	0	0.000	34.328	0.000
116.7	3.75	0	0.000	52.734	0.000
133.3	4.25	0	0.000	76.766	0.000
150.0	4.75	0	0.000	107.172	0.000
166.7	5.25	0	0.000	144.703	0.000
183.3	5.75	0	0.000	190.109	0.000
200.0	6.25	0	0.000	244.141	0.000
216.7	6.75	0	0.000	307.547	0.000
233.3	7.25	0	0.000	381.078	0.000
250.0	7.75	0	0.000	465.484	0.000
266.7	8.25	0	0.000	561.516	0.000
283.3	8.75	0	0.000	669.922	0.000
300.0	9.25	0	0.000	791.453	0.000
316.7	9.75	0	0.000	926.859	0.000
333.3	10.25	0	0.000	1076.891	0.000
350.0	10.75	0	0.000	1242.297	0.000
366.7	11.25	0	0.000	1423.828	0.000
383.3	11.75	0	0.000	1622.234	0.000
400.0	12.25	0	0.000	1838.266	0.000
416.7	12.75	0	0.000	2072.672	0.000
433.3	13.25	0	0.000	2326.203	0.000
450.0	13.75	0	0.000	2599.609	0.000
466.7	14.25	0	0.000	2893.641	0.000
483.3	14.75	0	0.000	3209.047	0.000
500.0	15.25	0	0.000	3546.578	0.000
	SUM=	16		SUM=	0.518
			Equivalent Stress = [SUM (Pi)* Sri^3]^(1/3) =		0.803 ksi
			Equivalent Number of Cycles Per Year =		5,840

Table 2. Miner's Equation to Find Equivalent Stress for Strain Gage I6581.

Range (ustrain)	Mid-Stress in Bins, Sri (ksi)	Number of Counts	Proportion of Stress Cycles (Pi)	(Mid-Stress in Bins)^3	Pi*Sri^3
underflow	0.00	0	0.000	0.000	0.000
0.0	0.25	0	0.000	0.016	0.000
16.7	0.75	1137	0.535	0.422	0.226
33.3	1.25	786	0.370	1.953	0.722
50.0	1.75	179	0.084	5.359	0.451
66.7	2.25	12	0.006	11.391	0.064
83.3	2.75	2	0.001	20.797	0.020
100.0	3.25	2	0.001	34.328	0.032
116.7	3.75	0	0.000	52.734	0.000
133.3	4.25	2	0.001	76.766	0.072
150.0	4.75	0	0.000	107.172	0.000
166.7	5.25	1	0.000	144.703	0.068
183.3	5.75	0	0.000	190.109	0.000
200.0	6.25	0	0.000	244.141	0.000
216.7	6.75	1	0.000	307.547	0.145
233.3	7.25	1	0.000	381.078	0.179
250.0	7.75	0	0.000	465.484	0.000
266.7	8.25	0	0.000	561.516	0.000
283.3	8.75	0	0.000	669.922	0.000
300.0	9.25	1	0.000	791.453	0.372
316.7	9.75	0	0.000	926.859	0.000
333.3	10.25	0	0.000	1076.891	0.000
350.0	10.75	0	0.000	1242.297	0.000
366.7	11.25	0	0.000	1423.828	0.000
383.3	11.75	0	0.000	1622.234	0.000
400.0	12.25	1	0.000	1838.266	0.865
416.7	12.75	0	0.000	2072.672	0.000
433.3	13.25	0	0.000	2326.203	0.000
450.0	13.75	0	0.000	2599.609	0.000
466.7	14.25	1	0.000	2893.641	1.361
483.3	14.75	0	0.000	3209.047	0.000
500.0	15.25	0	0.000	3546.578	0.000
	SUM=	2126		SUM=	4.577
			Equivalent Stress = [SUM (Pi)* Sri^3]^(1/3) =		1.660 ksi
			Equivalent Number of Cycles Per Year =		773,864

Table 3. Miner's Equation to Find Equivalent Stress for Strain Gage I6582.

FIGURES

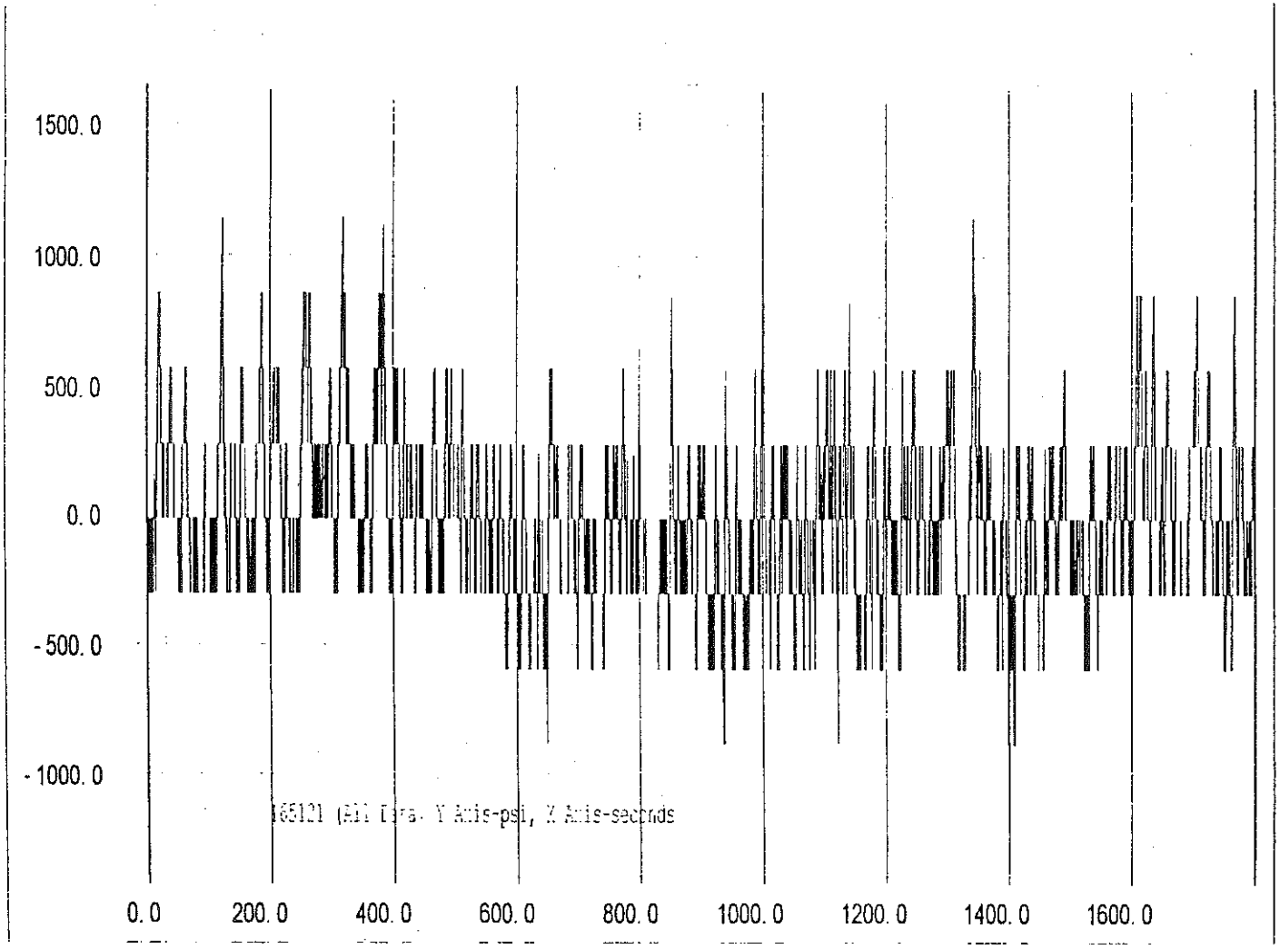

Figure 1. Live Stress Data for Strain Gage I65121.

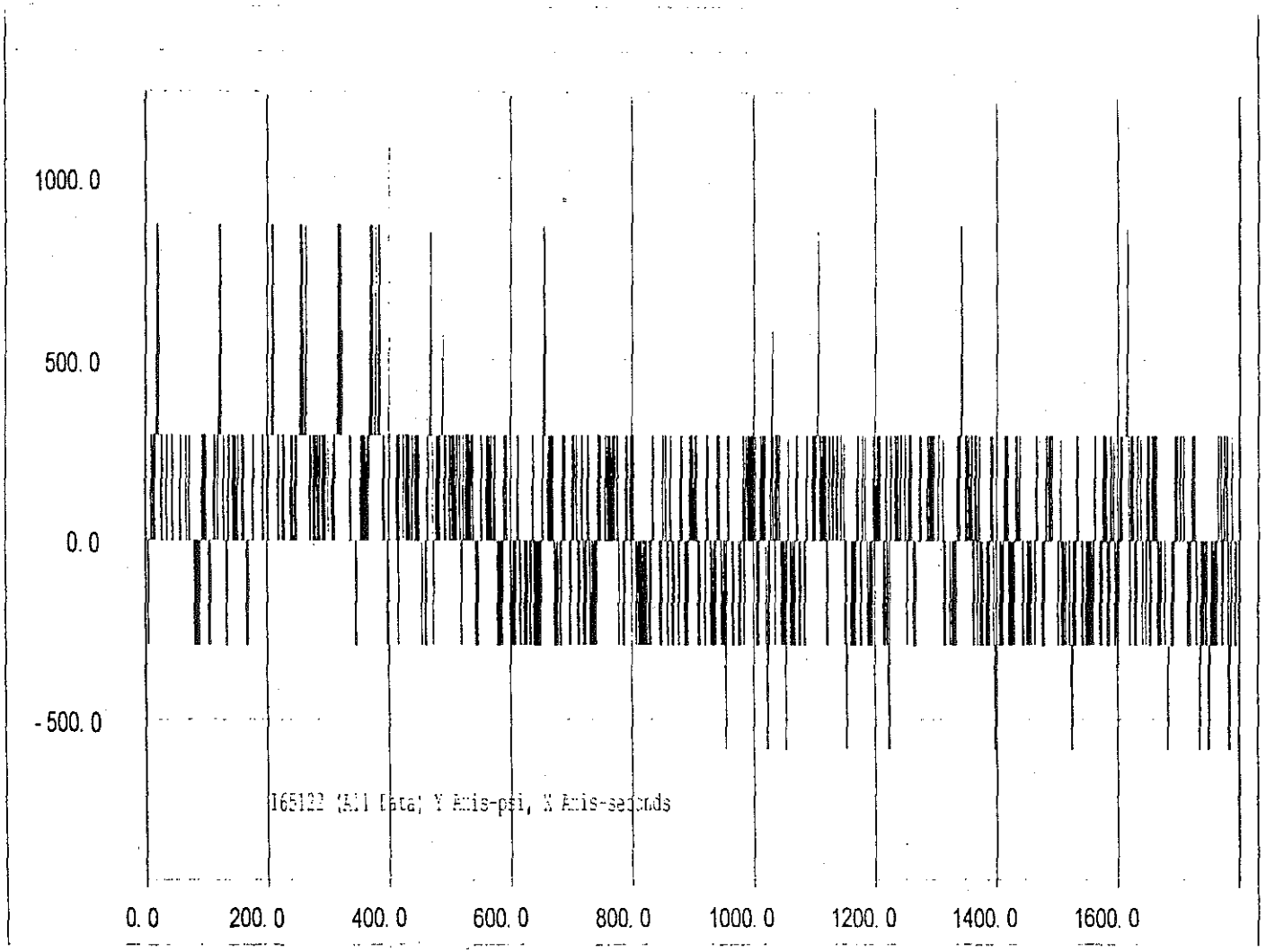

Figure 2. Live Stress Data for Strain Gage I65122.

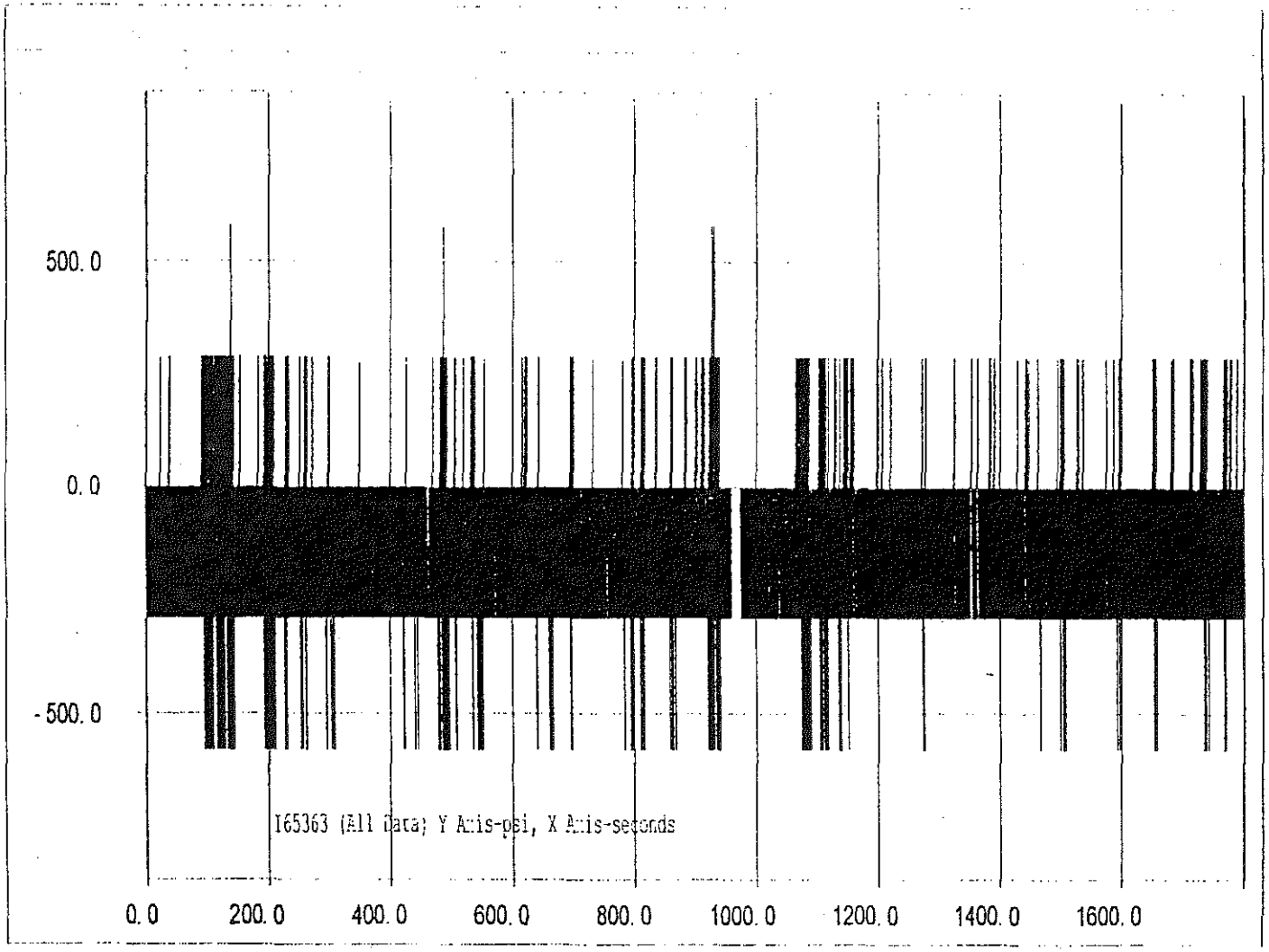

Figure 3. Live Stress Data for Strain Gage I65363.

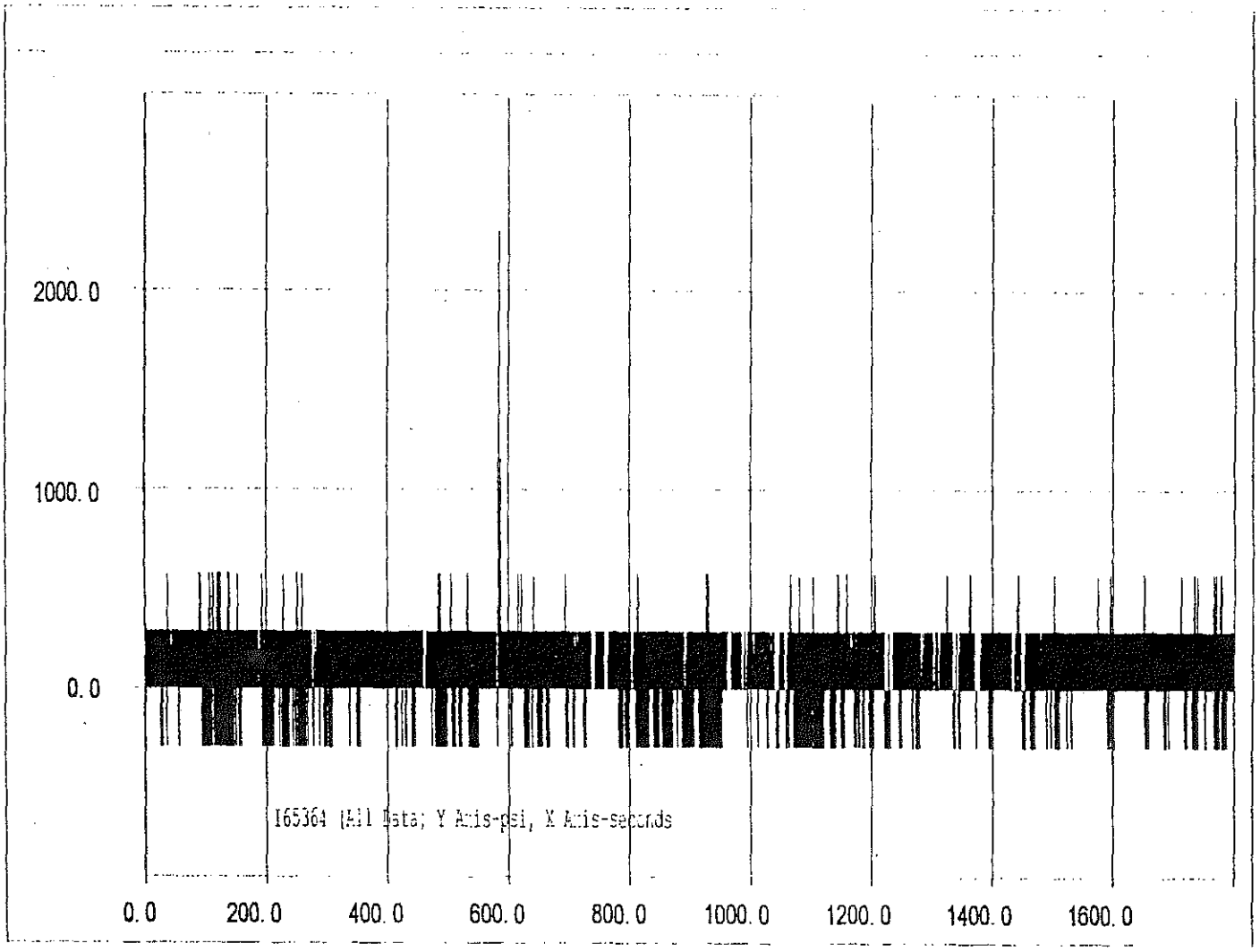

Figure 4. Live Stress Data for Strain Gage I65364.

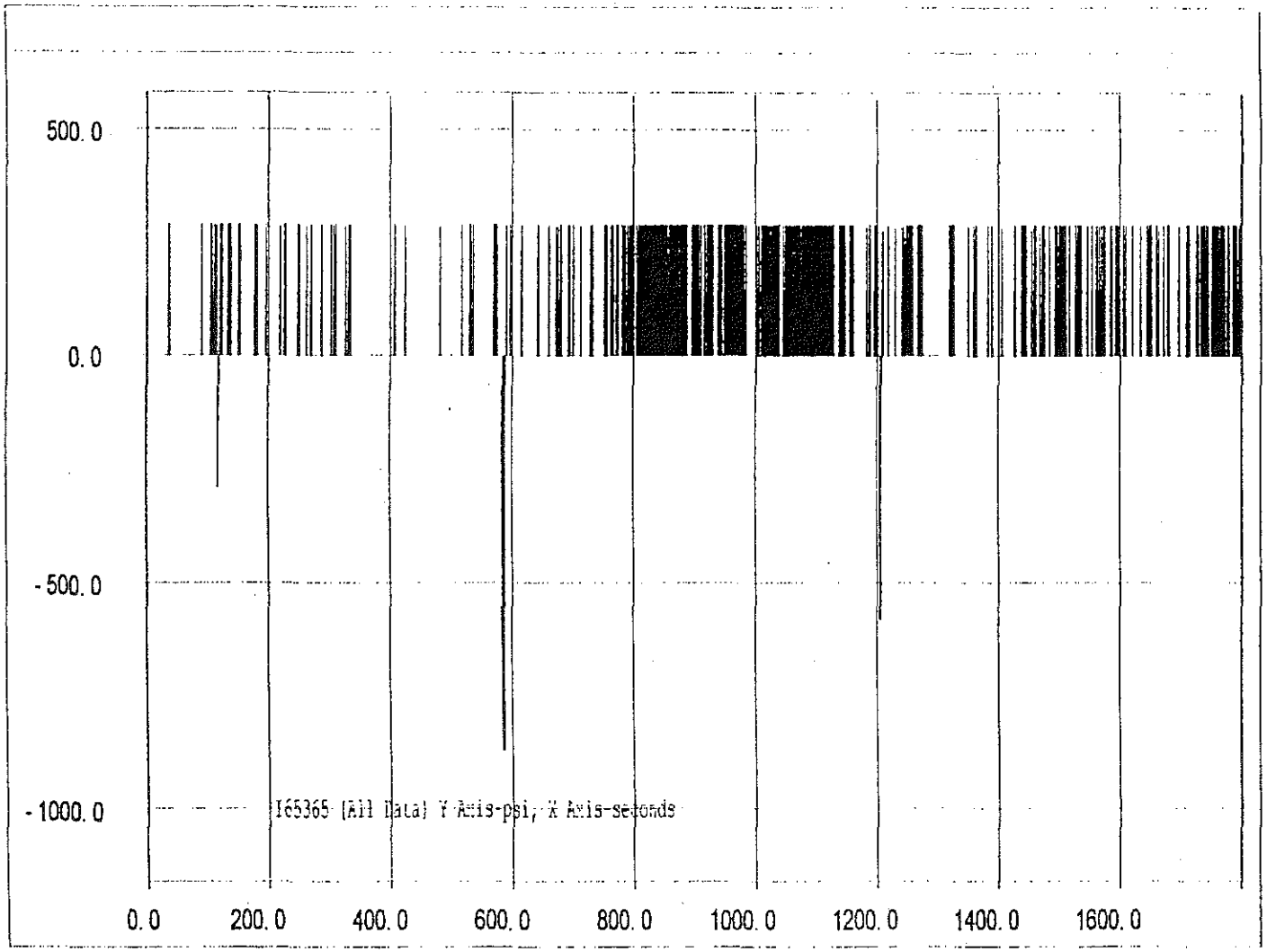

Figure 5. Live Stress Data for Strain Gage I65365.

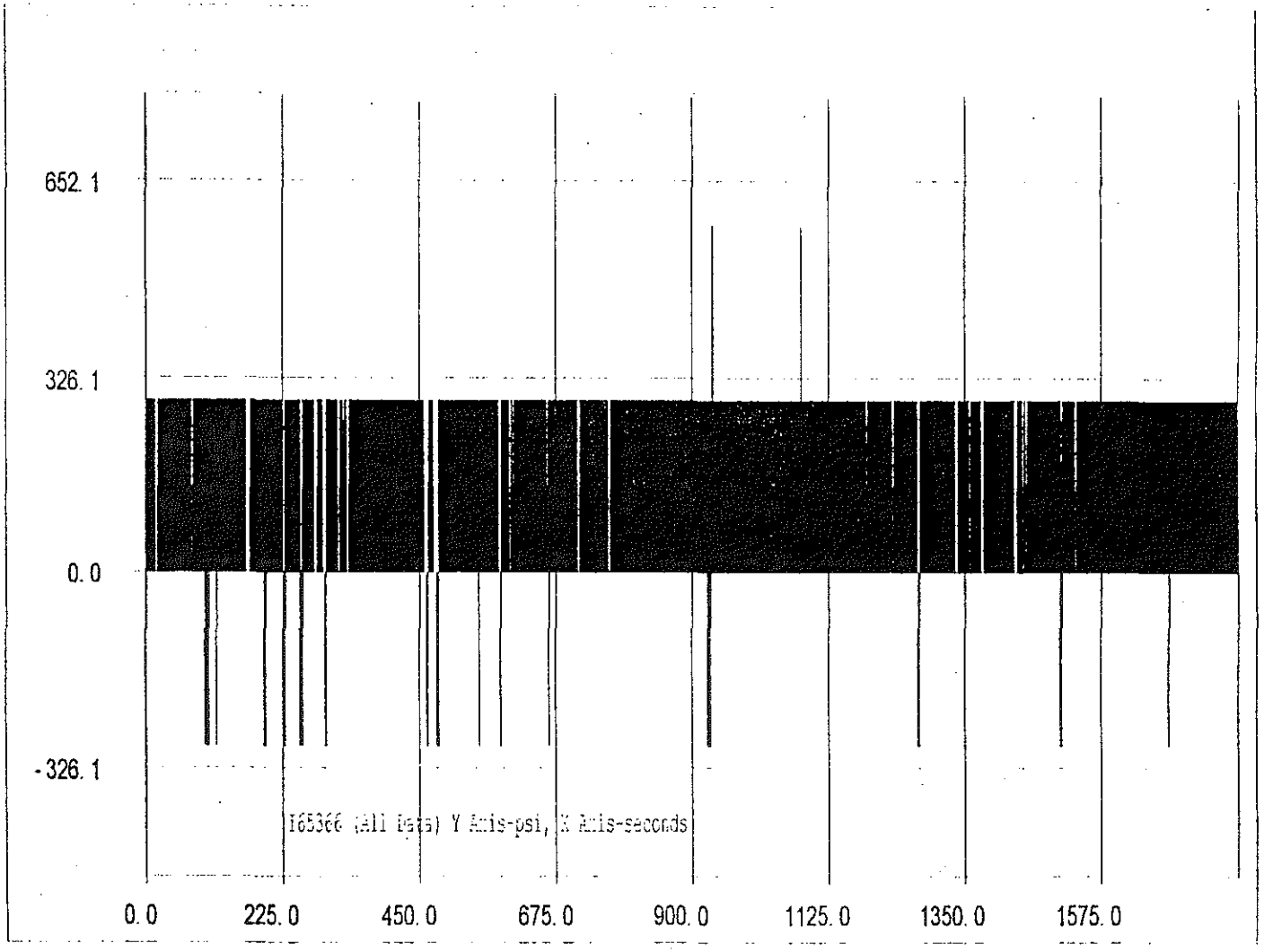

Figure 6. Live Stress Data for Strain Gage I65366.

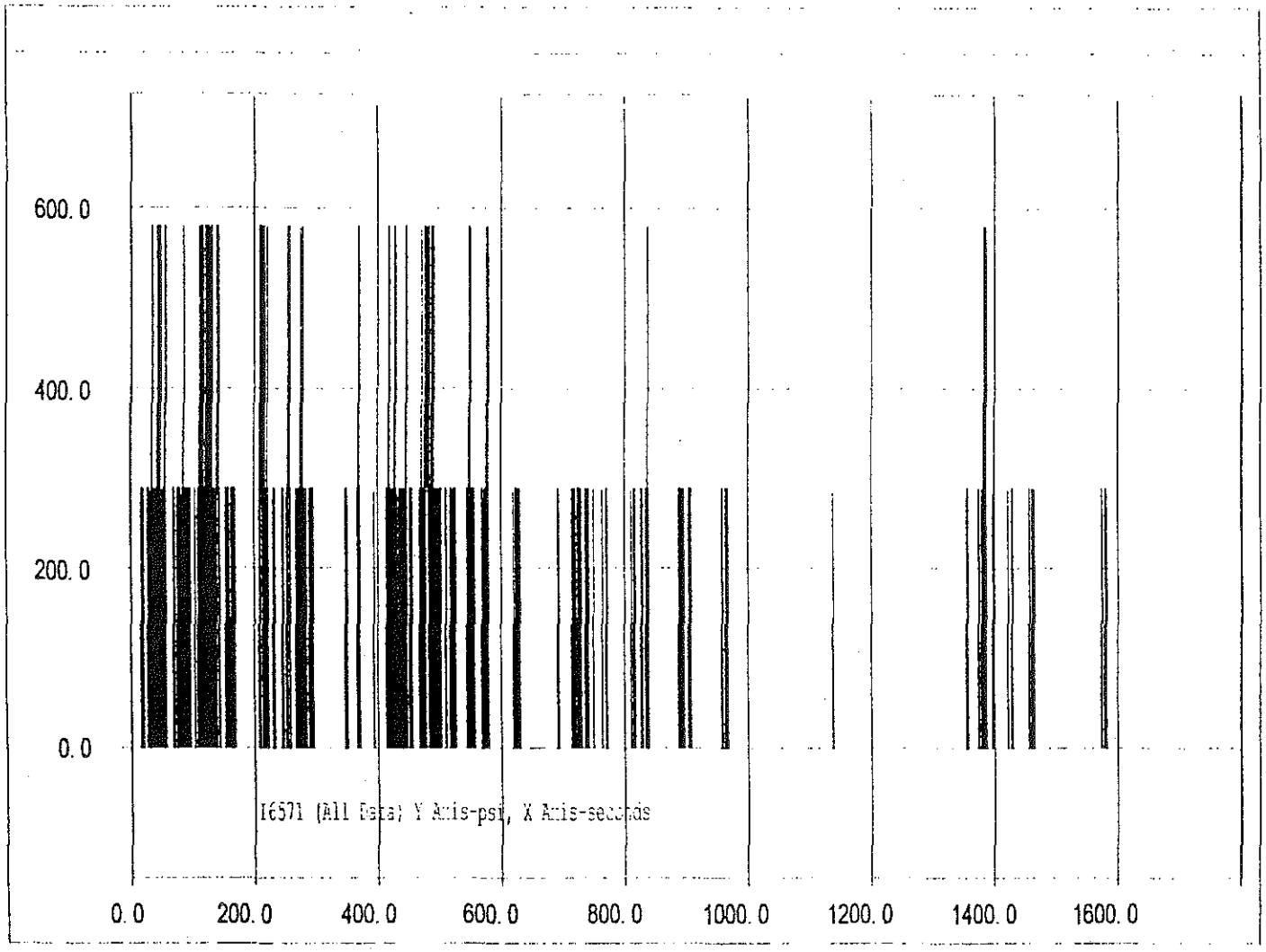

Figure 7. Live Stress Data for Strain Gage I6571.

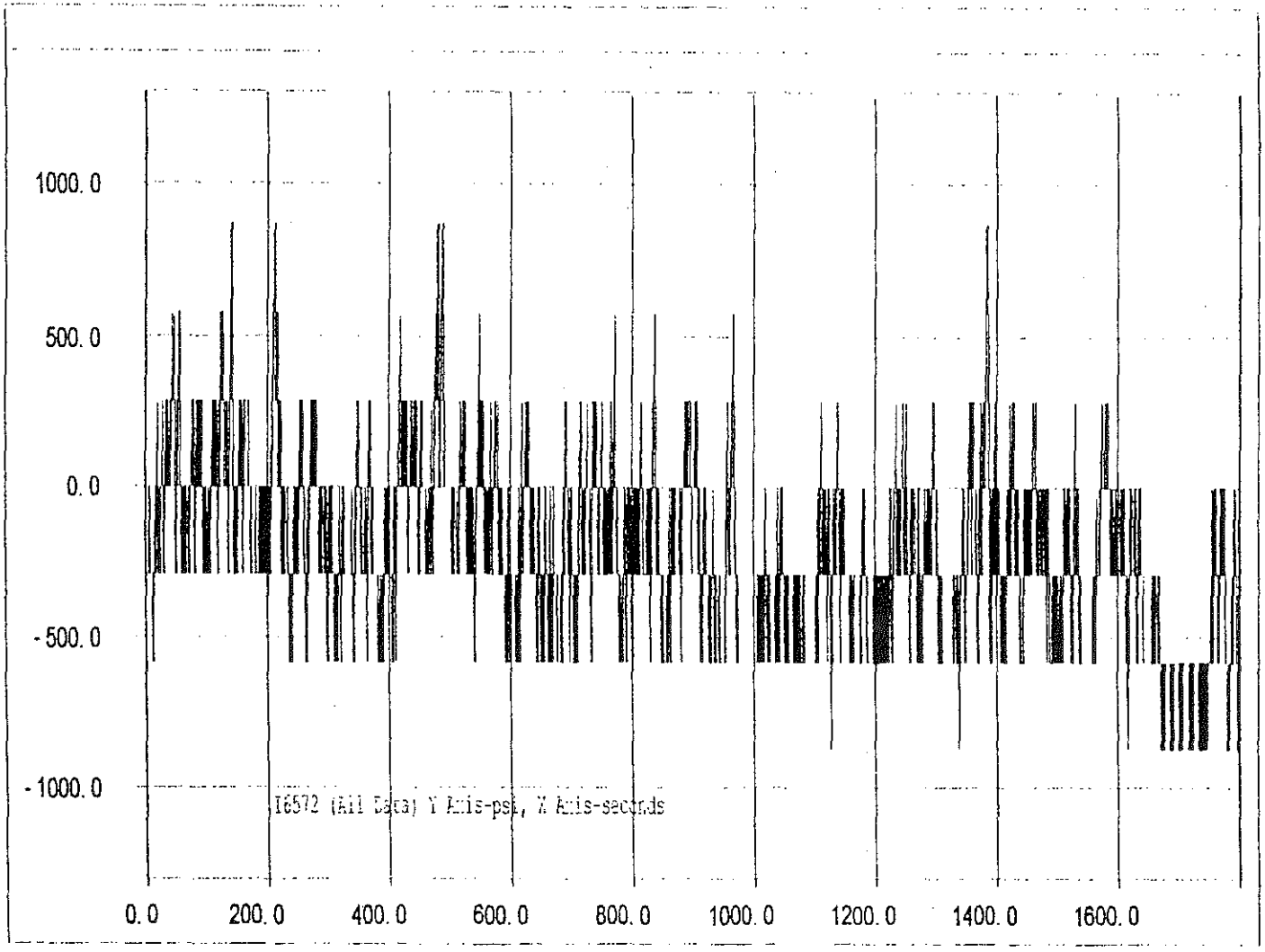

Figure 8. Live Stress Data for Strain Gage I6572.

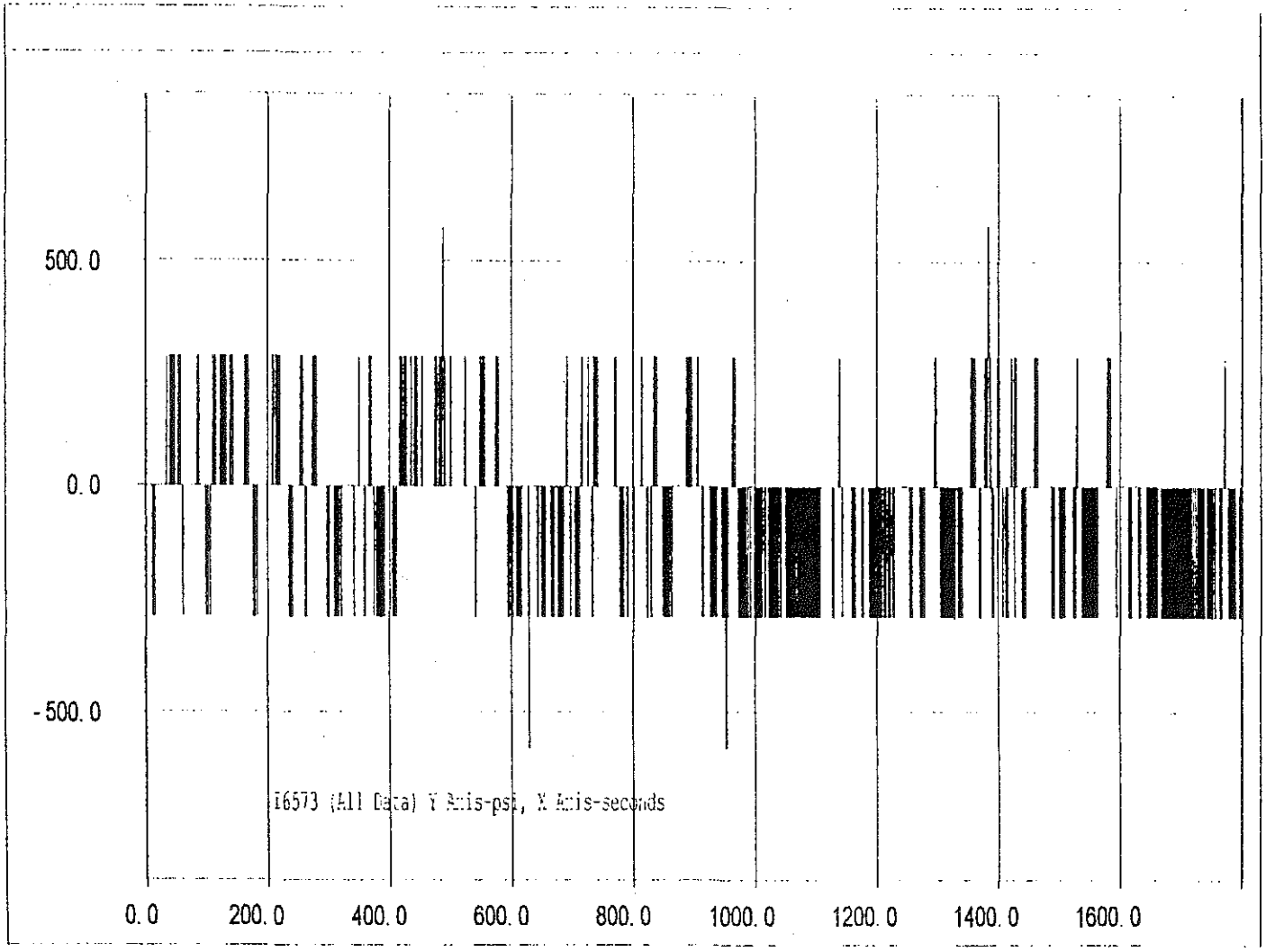

Figure 9. Live Stress Data for Strain Gage I6573.

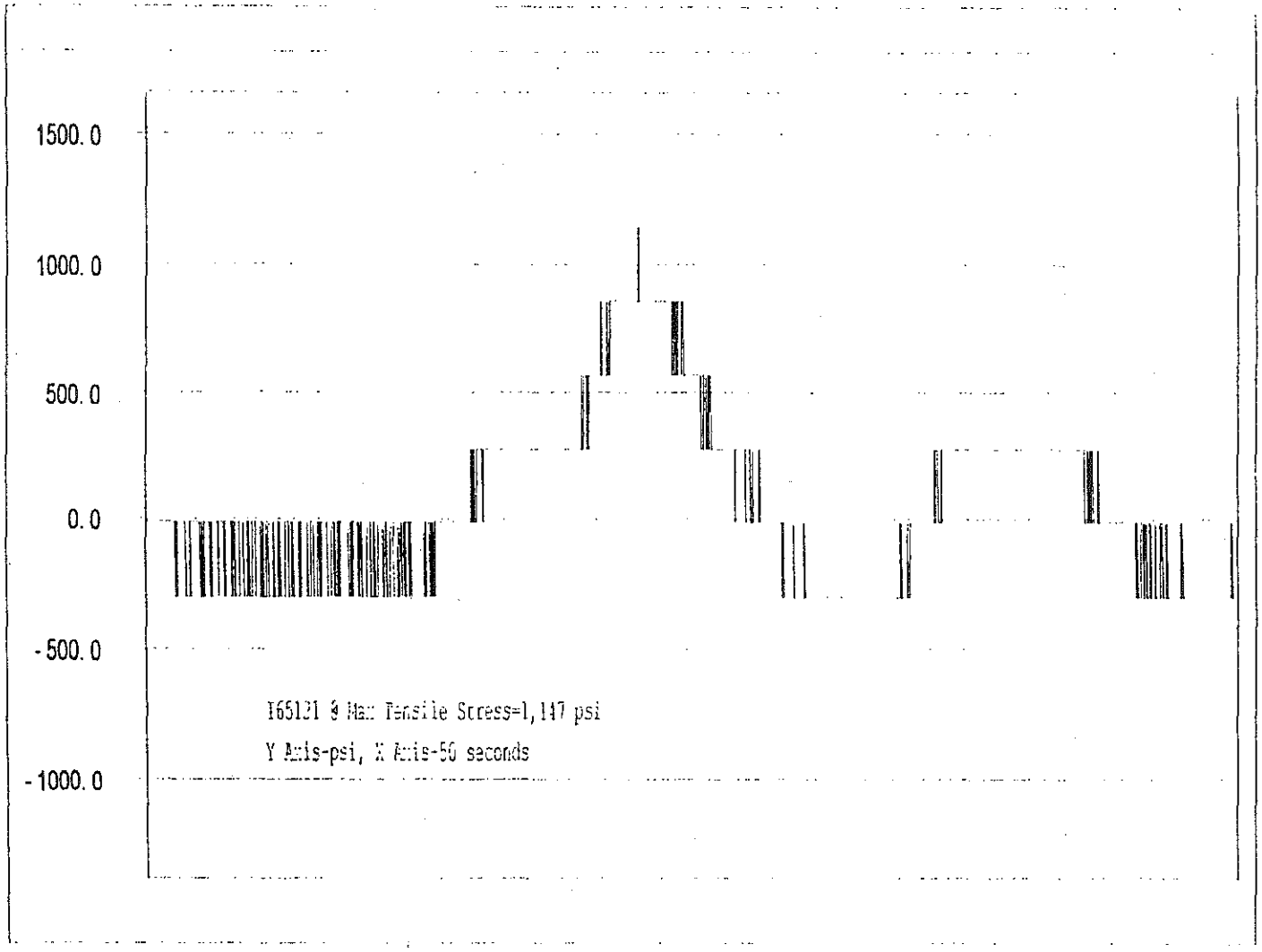

Figure 10. Maximum Tensile Live Stress for Strain Gage I65121.

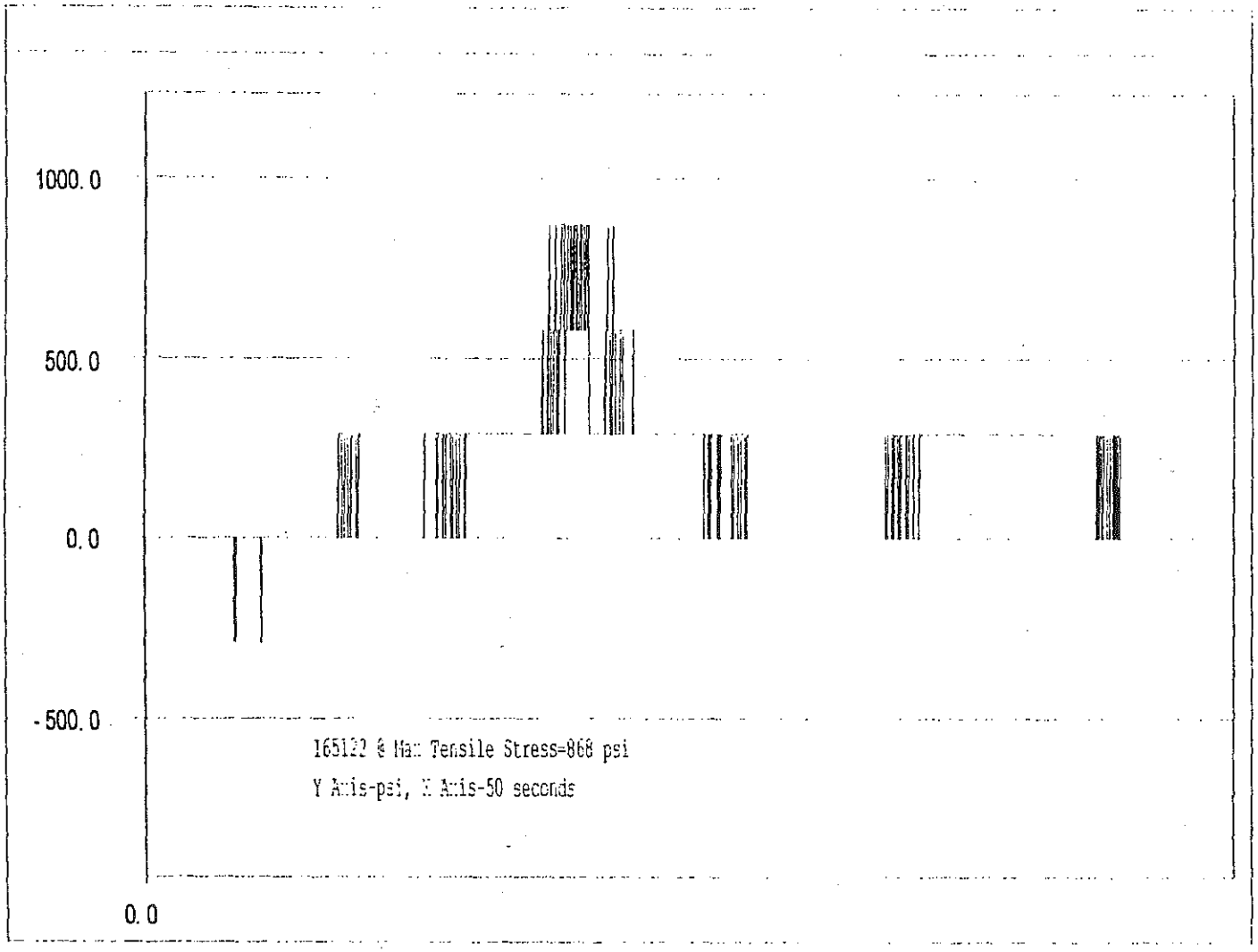

Figure 11. Maximum Tensile Live Stress for Strain Gage I65122.

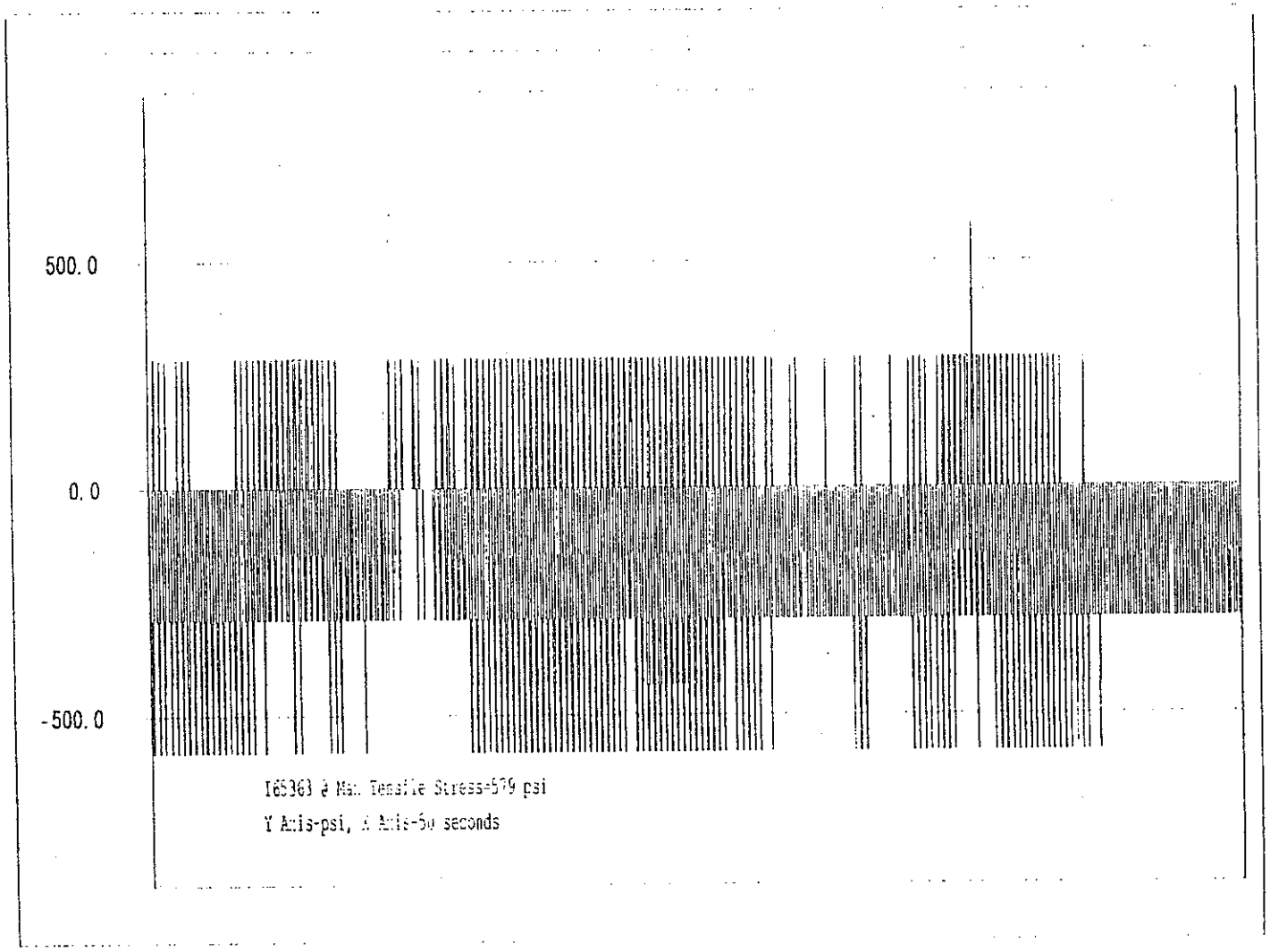

Figure 12. Maximum Tensile Live Stress for Strain Gage I65363.

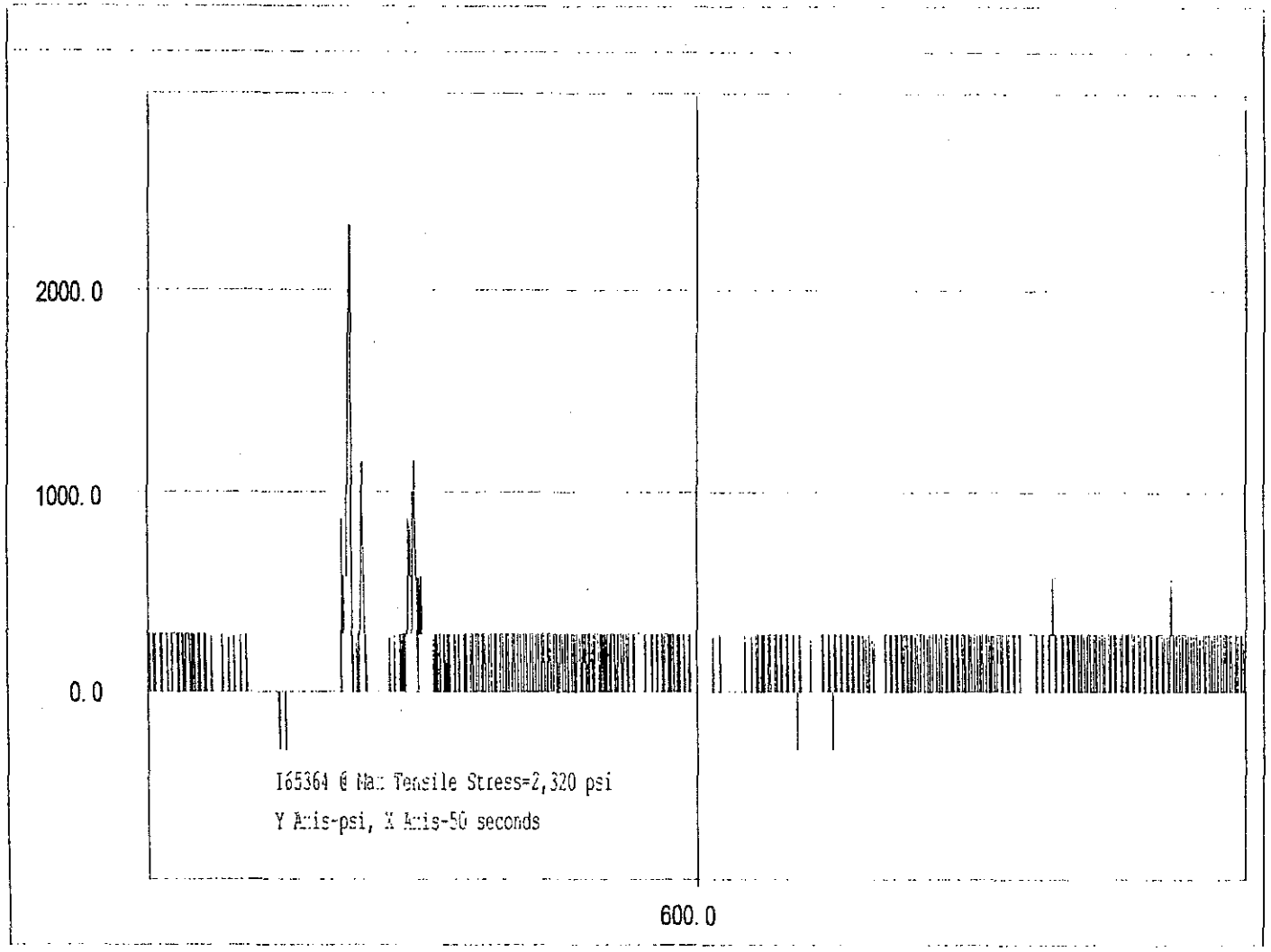

Figure 13. Maximum Tensile Live Stress for Strain Gage I65364.

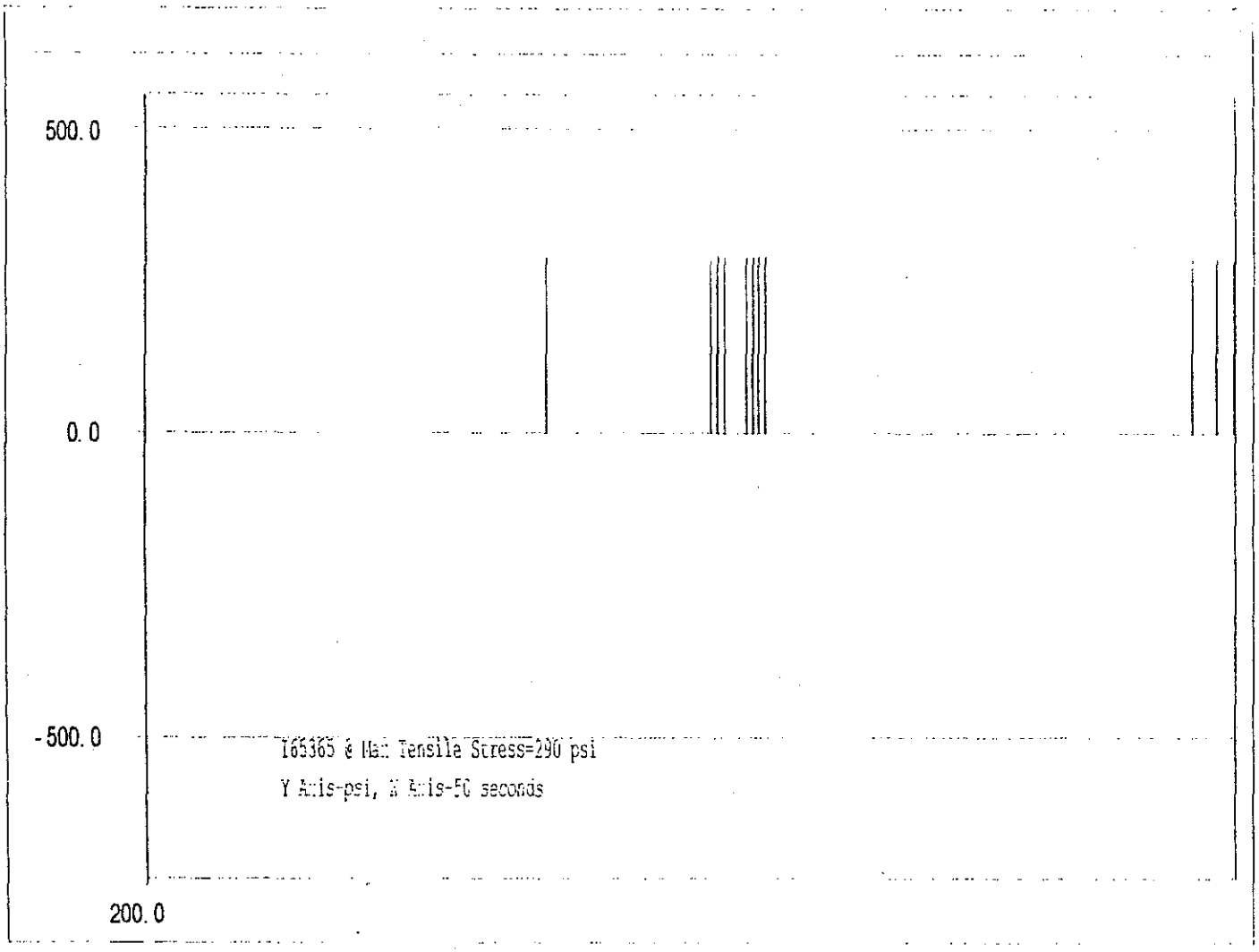

Figure 14. Maximum Tensile Live Stress for Strain Gage I65365.

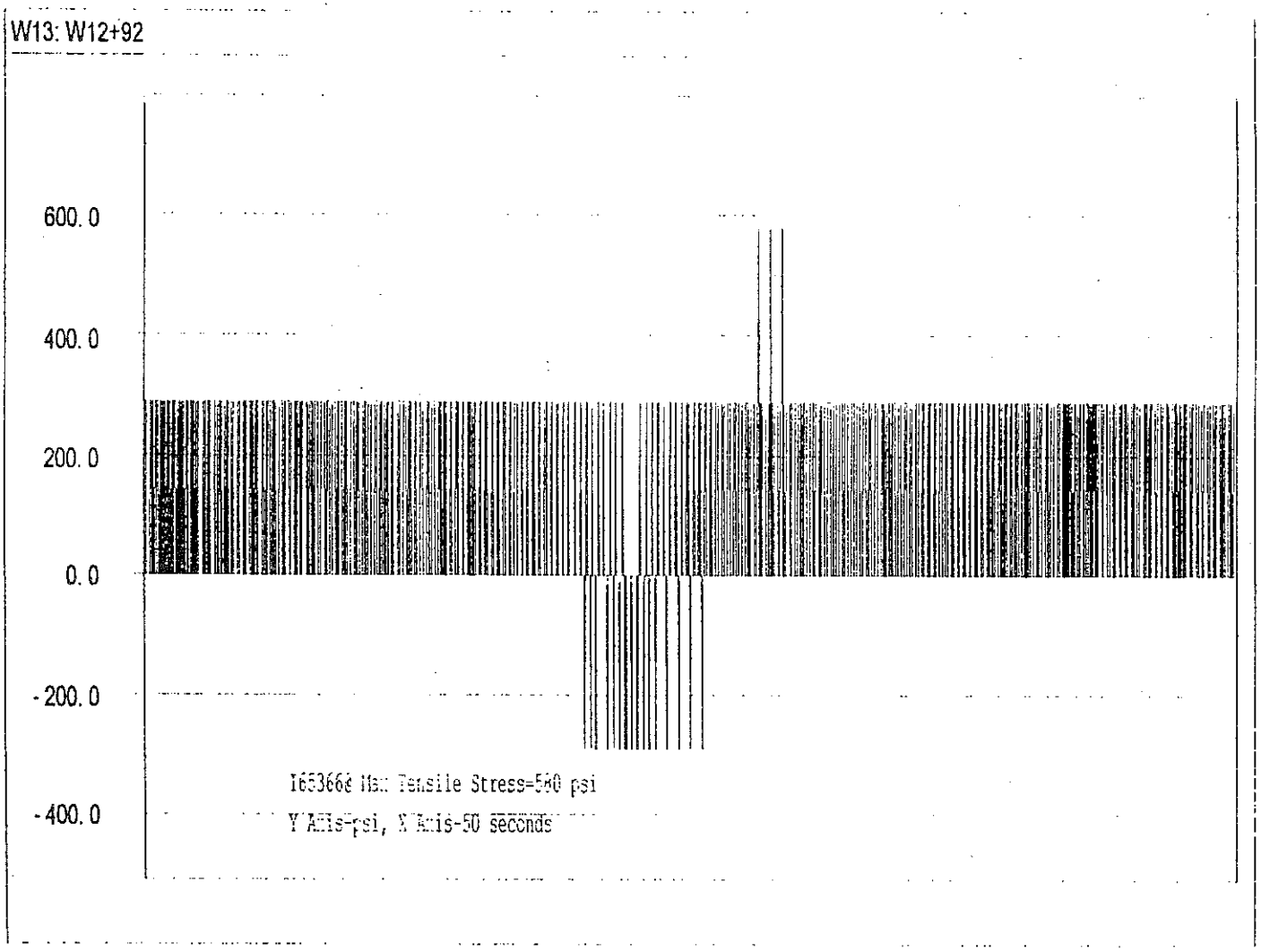

Figure 15. Maximum Tensile Live Stress for Strain Gage I65366.

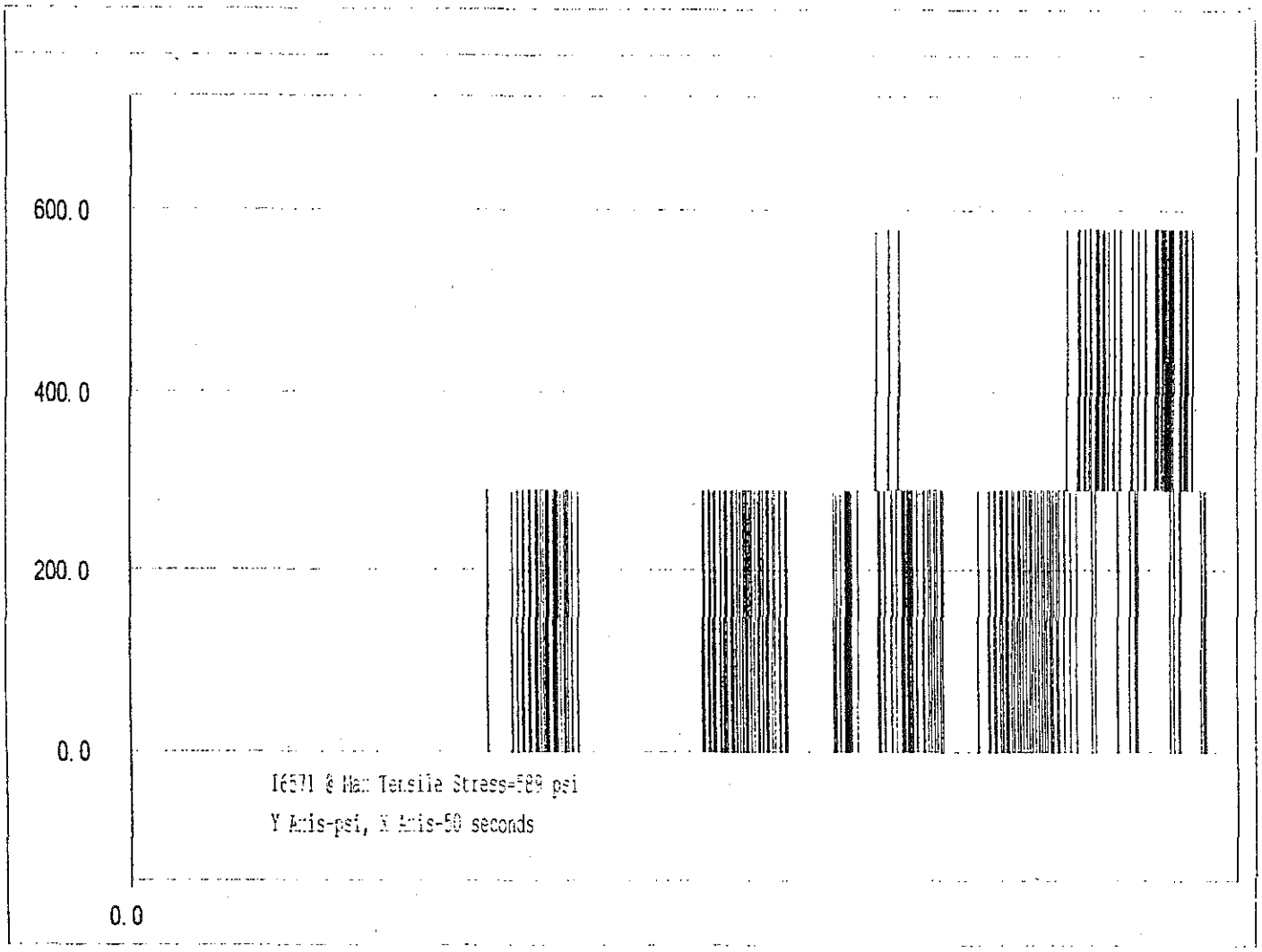

Figure 16. Maximum Tensile Live Stress for Strain Gage I6571.

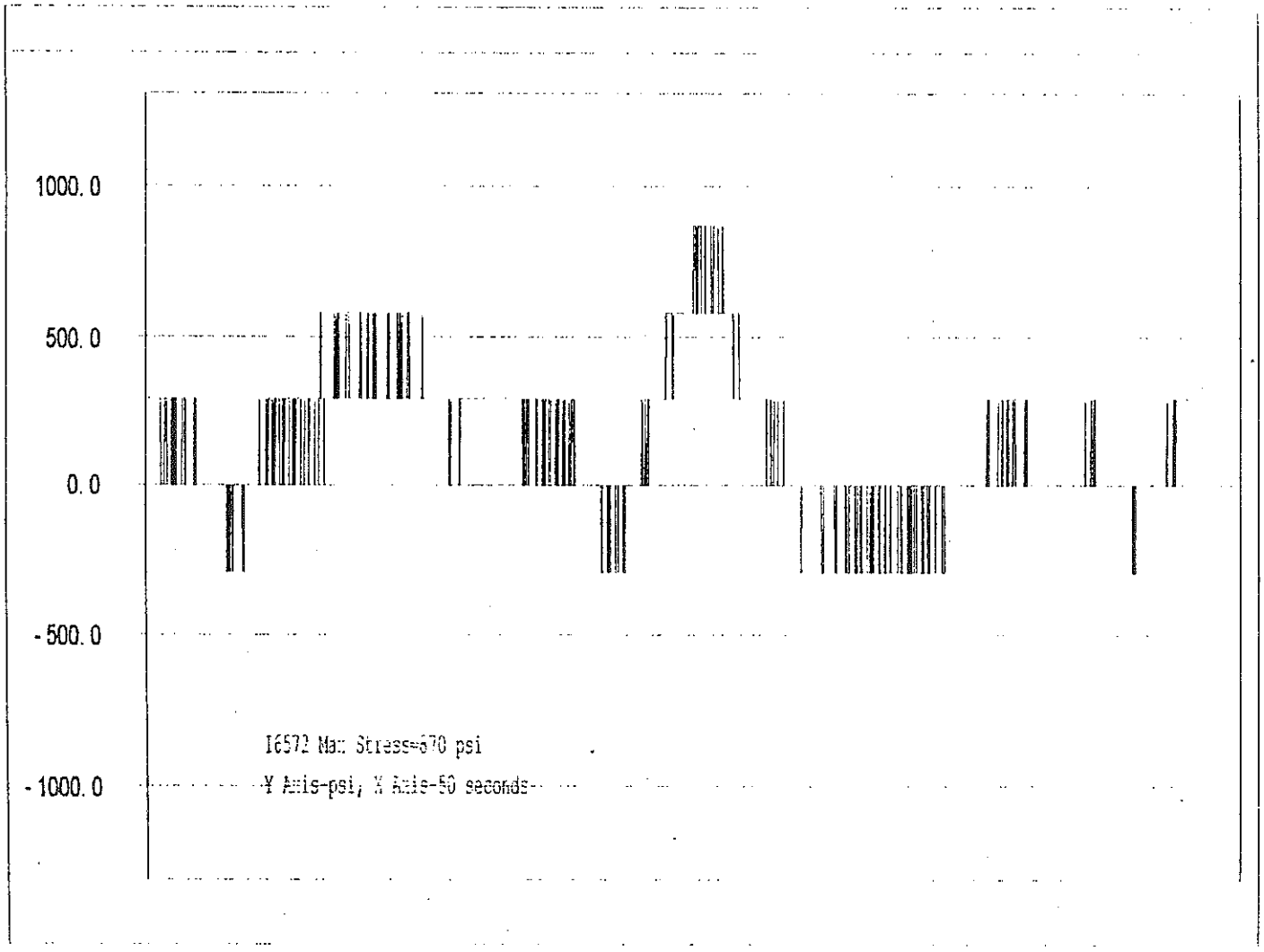

Figure 17. Maximum Tensile Live Stress for Strain Gage I6572.

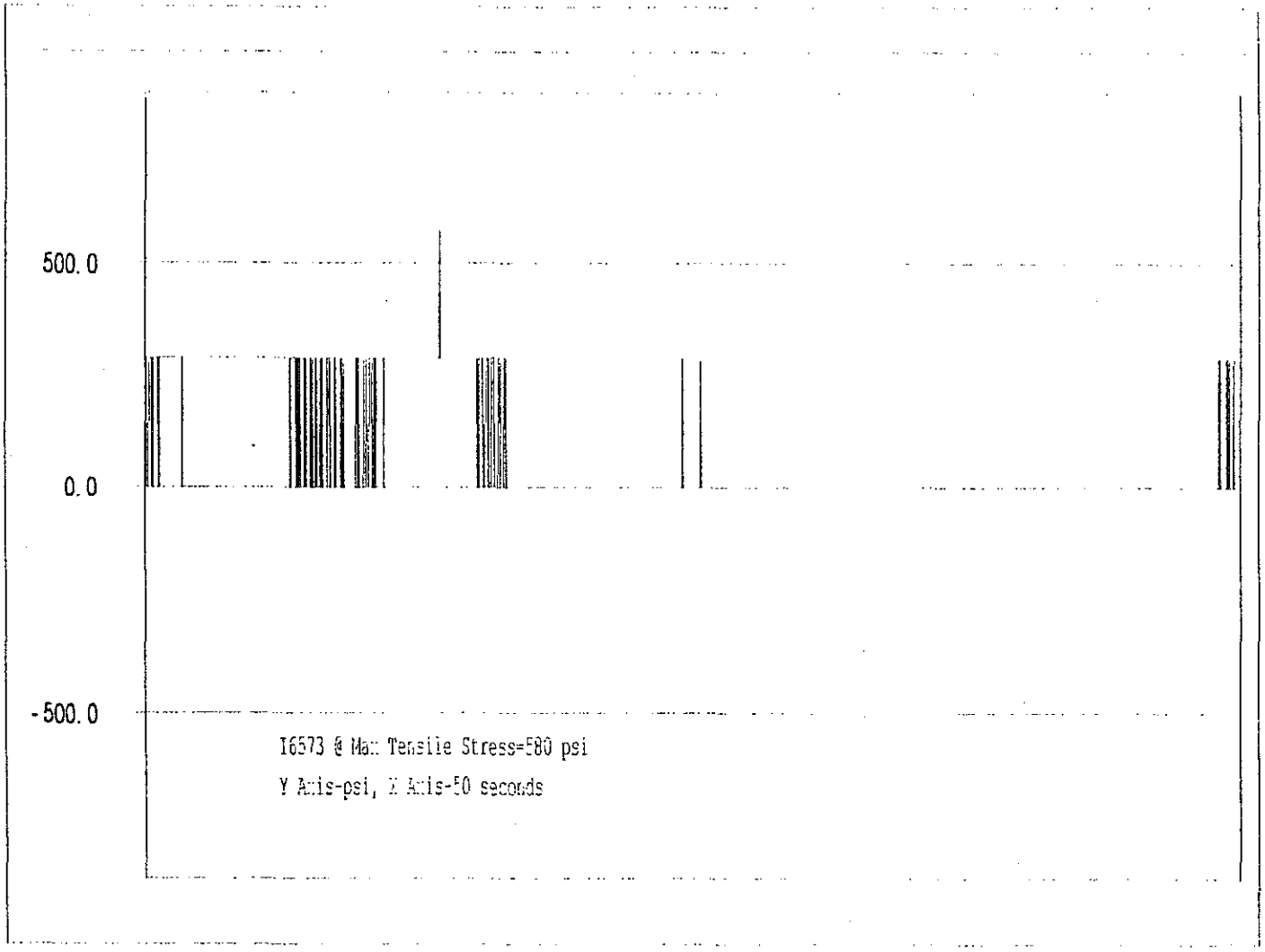

Figure 18. Maximum Tensile Live Stress for Strain Gage I6573.

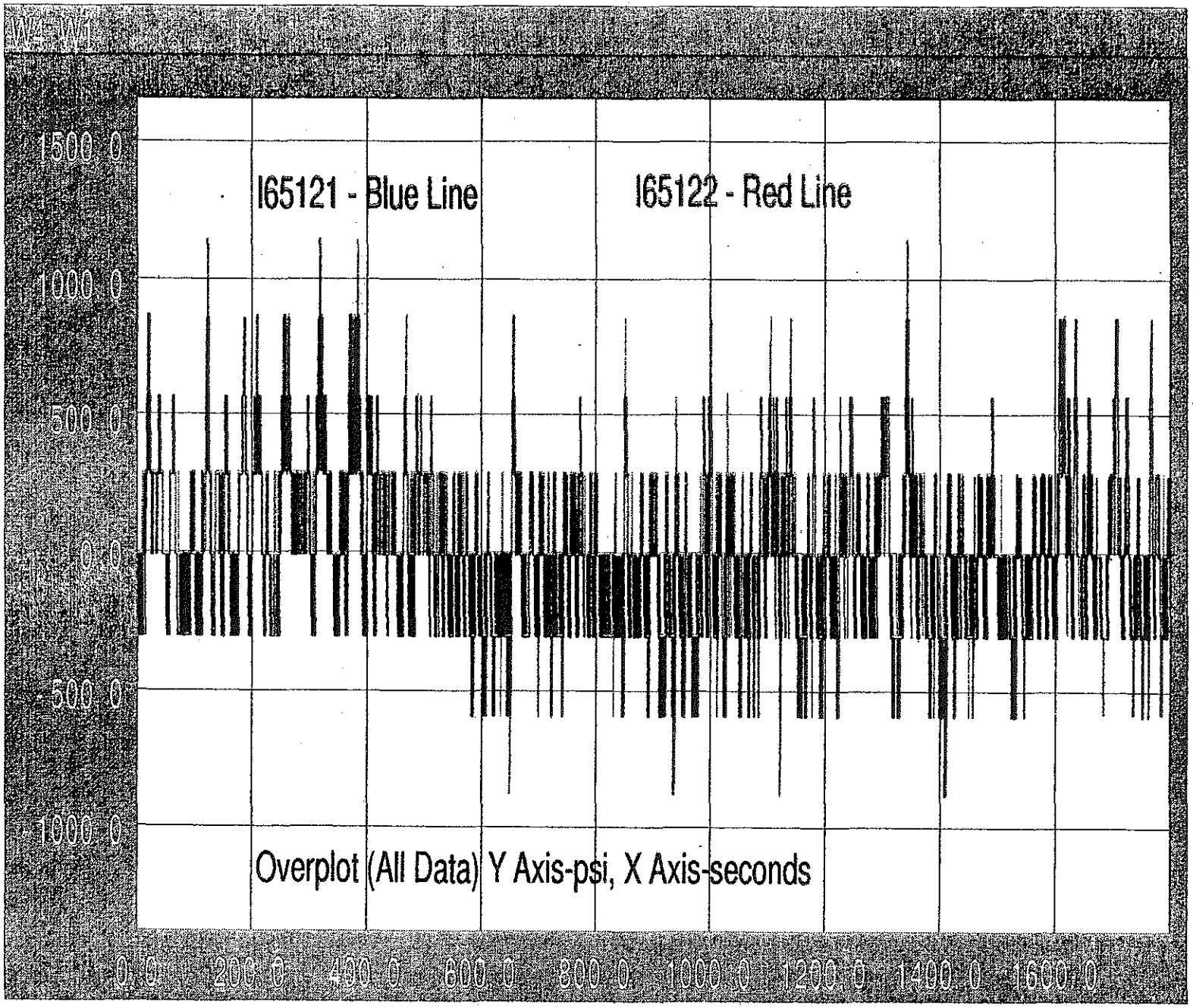

Figure 19. Overplot of Live Stresses for Strain Gages I65121 and I65122 (All Data).

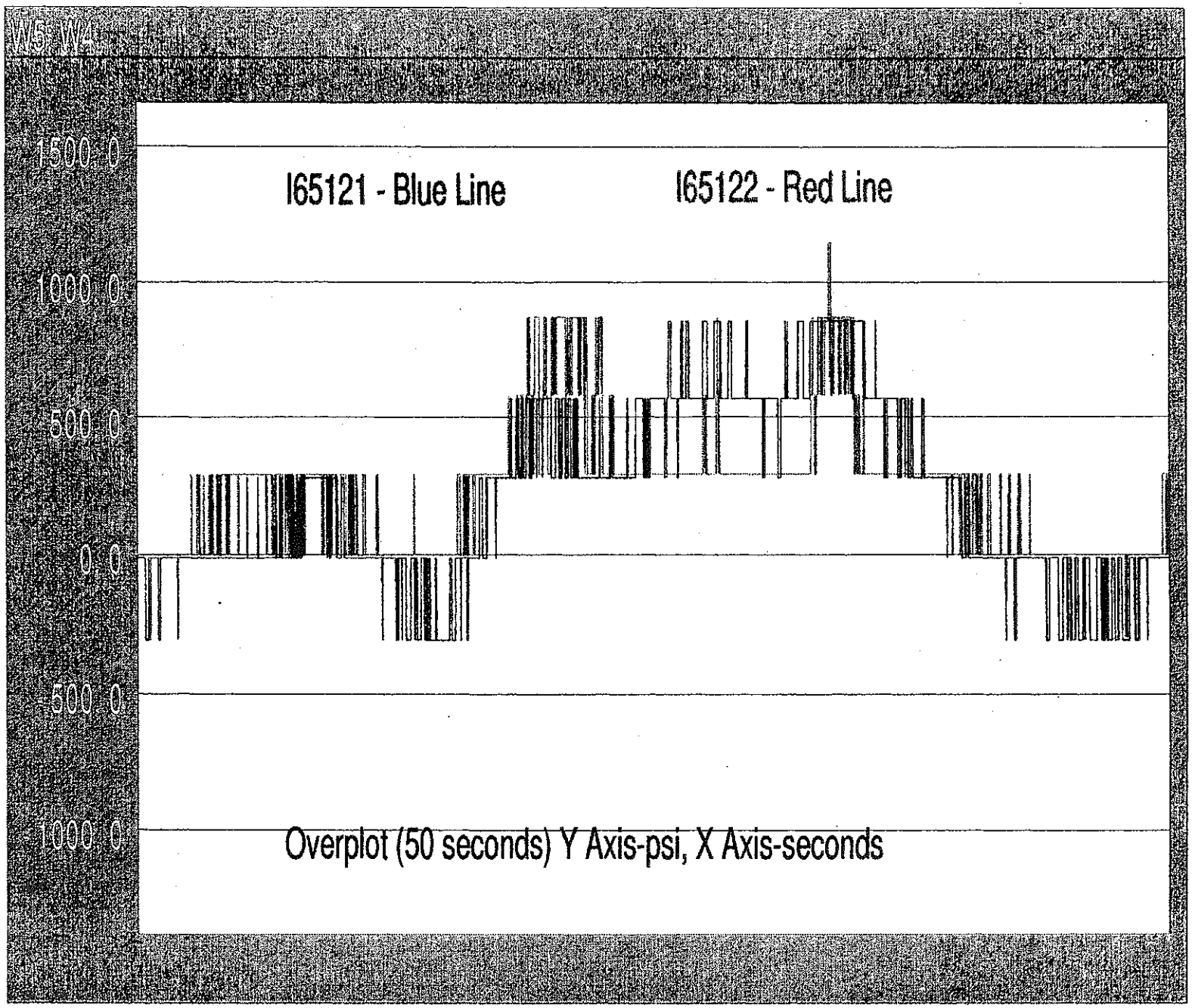

Figure 20. Overplot of Live Stresses for Strain Gages I65121 and I65122 (50 seconds).

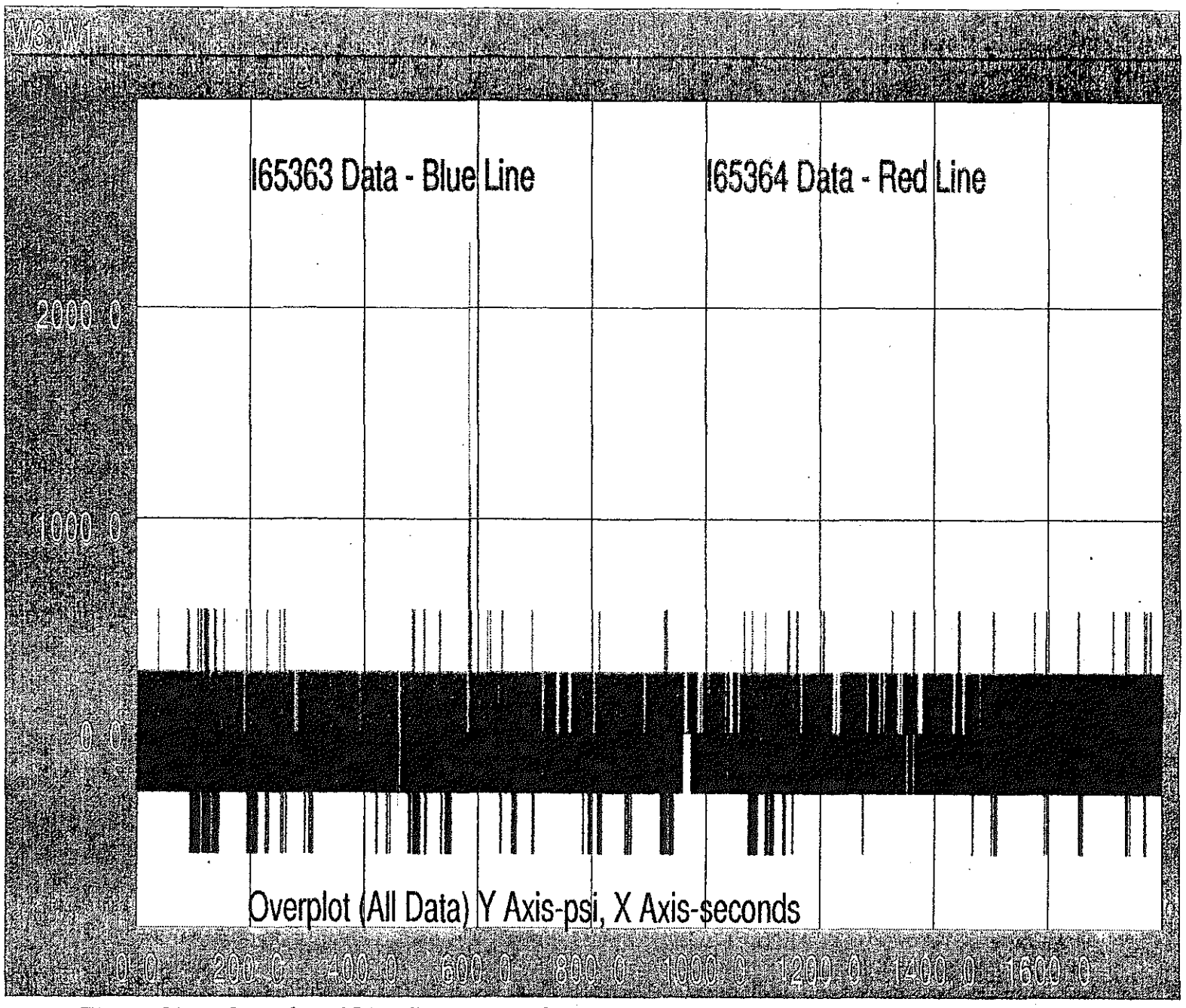

Figure 21. Overplot of Live Stresses for Strain Gages I65363 and I65364 (All Data).

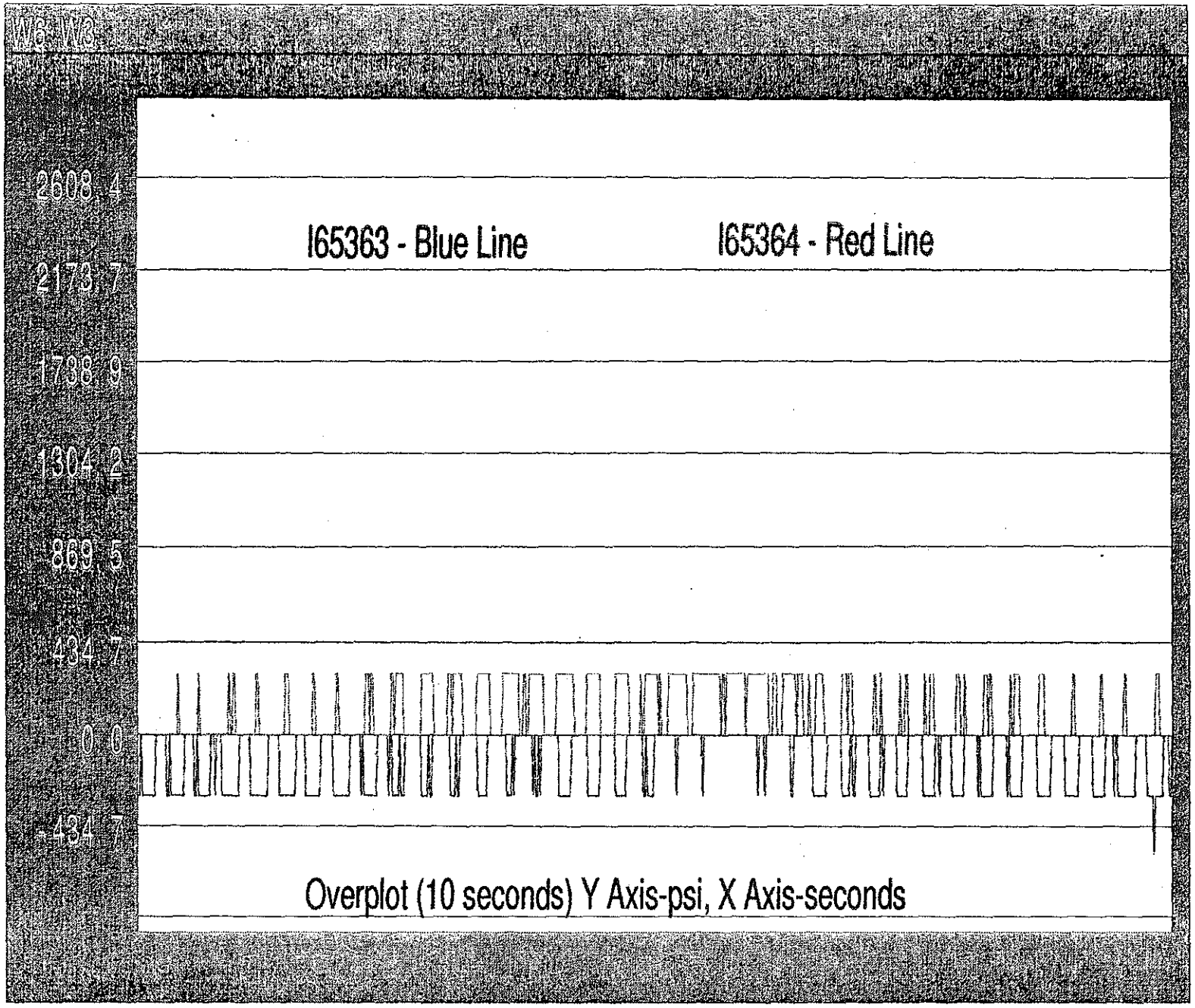

Figure 22. Overplot of Live Stresses for Strain Gages I65363 and I65364 (10 seconds).

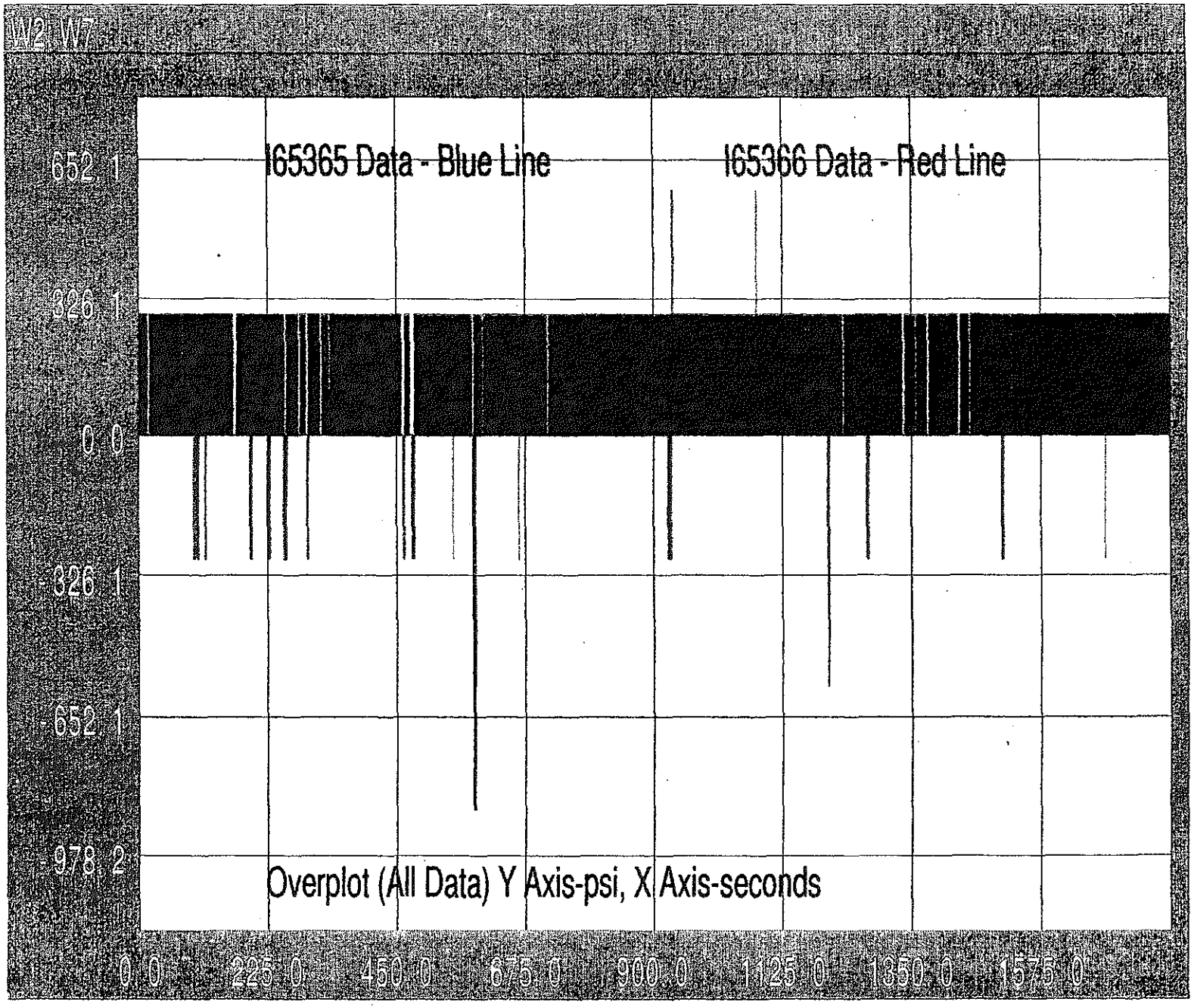

Figure 23. Overplot of Live Stresses for Strain Gages I65365 and I65366 (All Data).

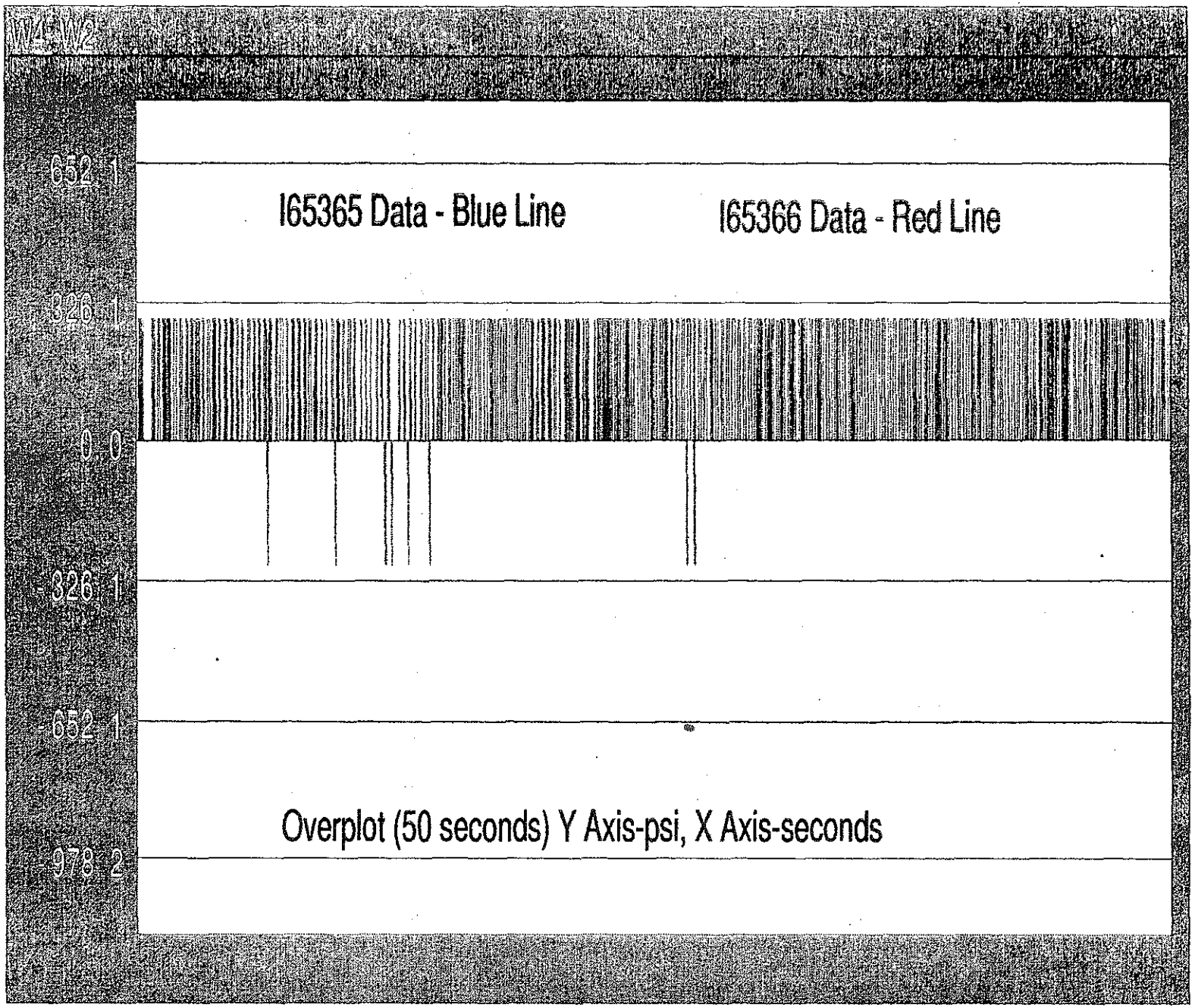

Figure 24. Overplot of Live Stresses for Strain Gages I65365 and I65366 (50 seconds).

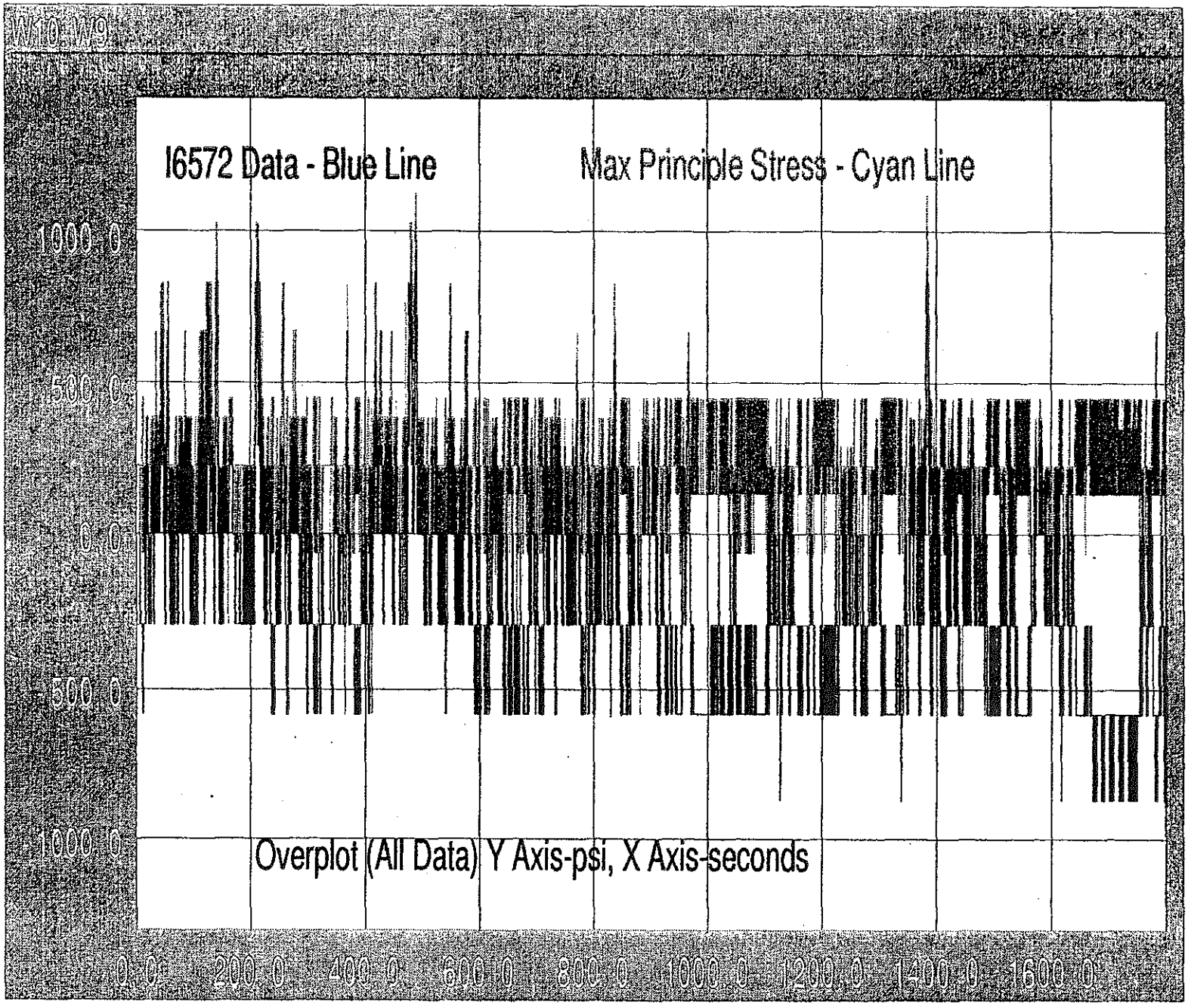

Figure 25. Overplot of Live Stress for Strain Gage I6572 and Maximum Principle Stress (All Data).

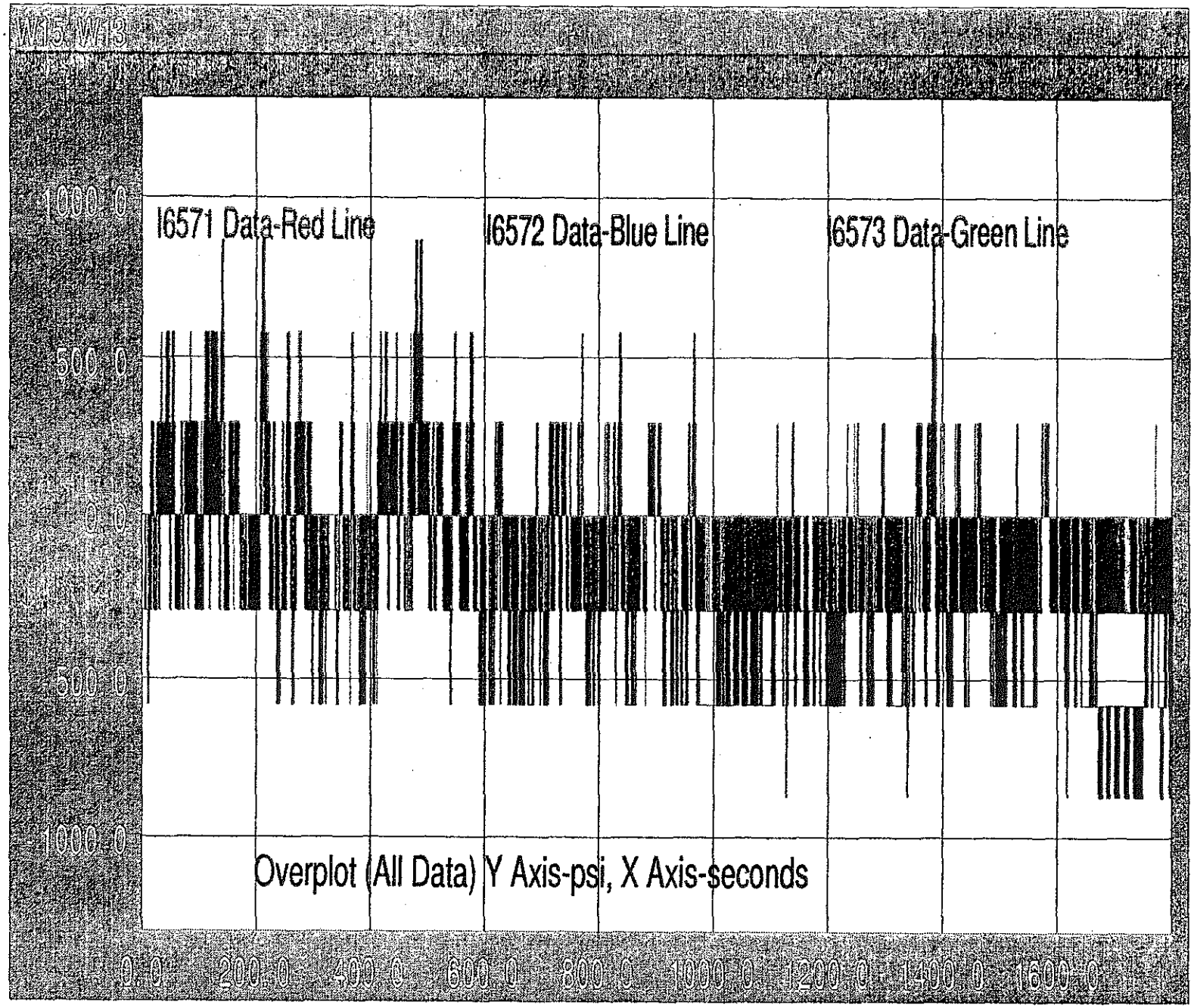

Figure 26. Overplot of Live Stresses for Strain Gages I6571, I6572 and I6573 (All Data).

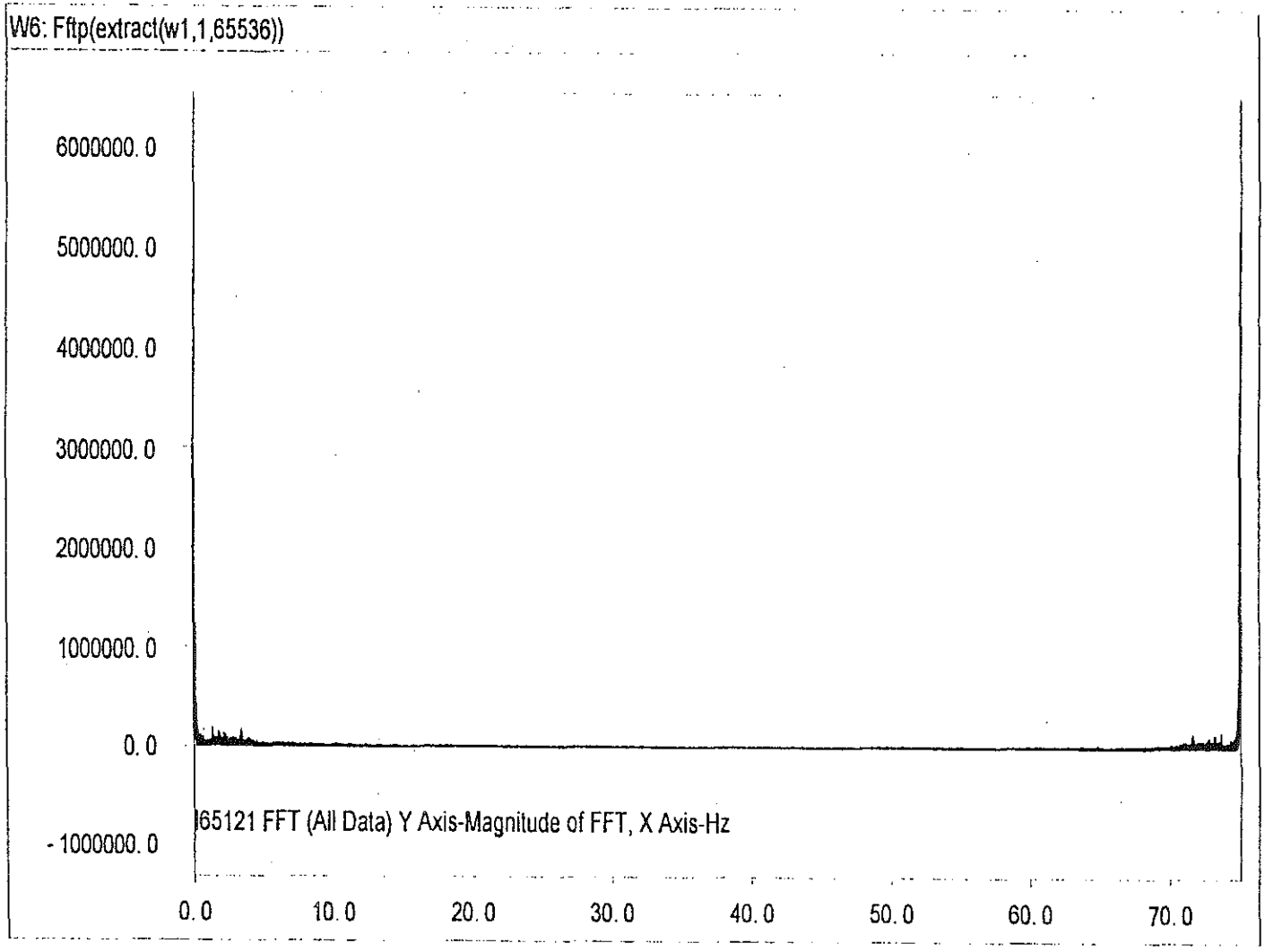

Figure 27. FFT for Live Stress Data from Strain Gage I65121.

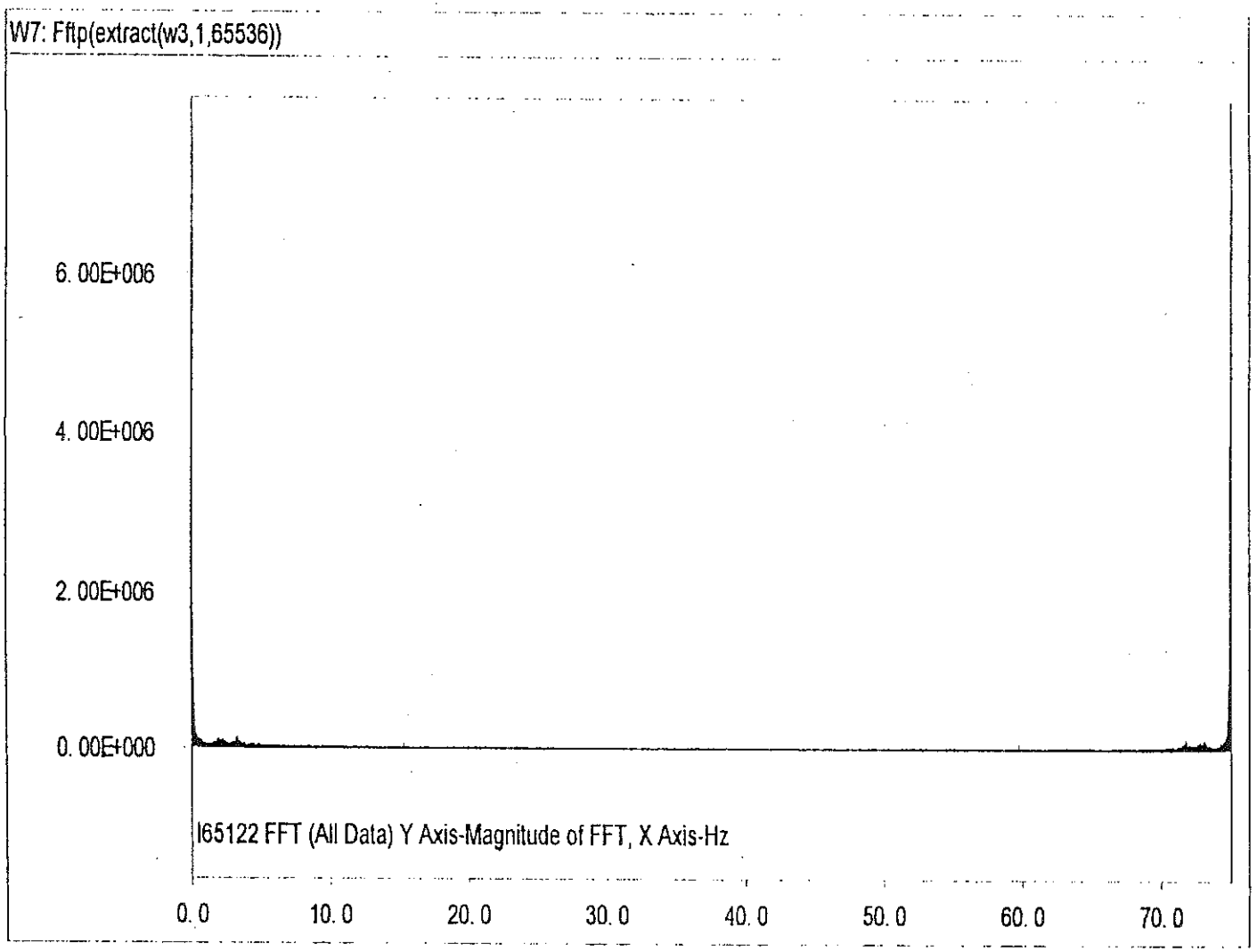

Figure 28. FFT for Live Stress Data from Strain Gage I65122.

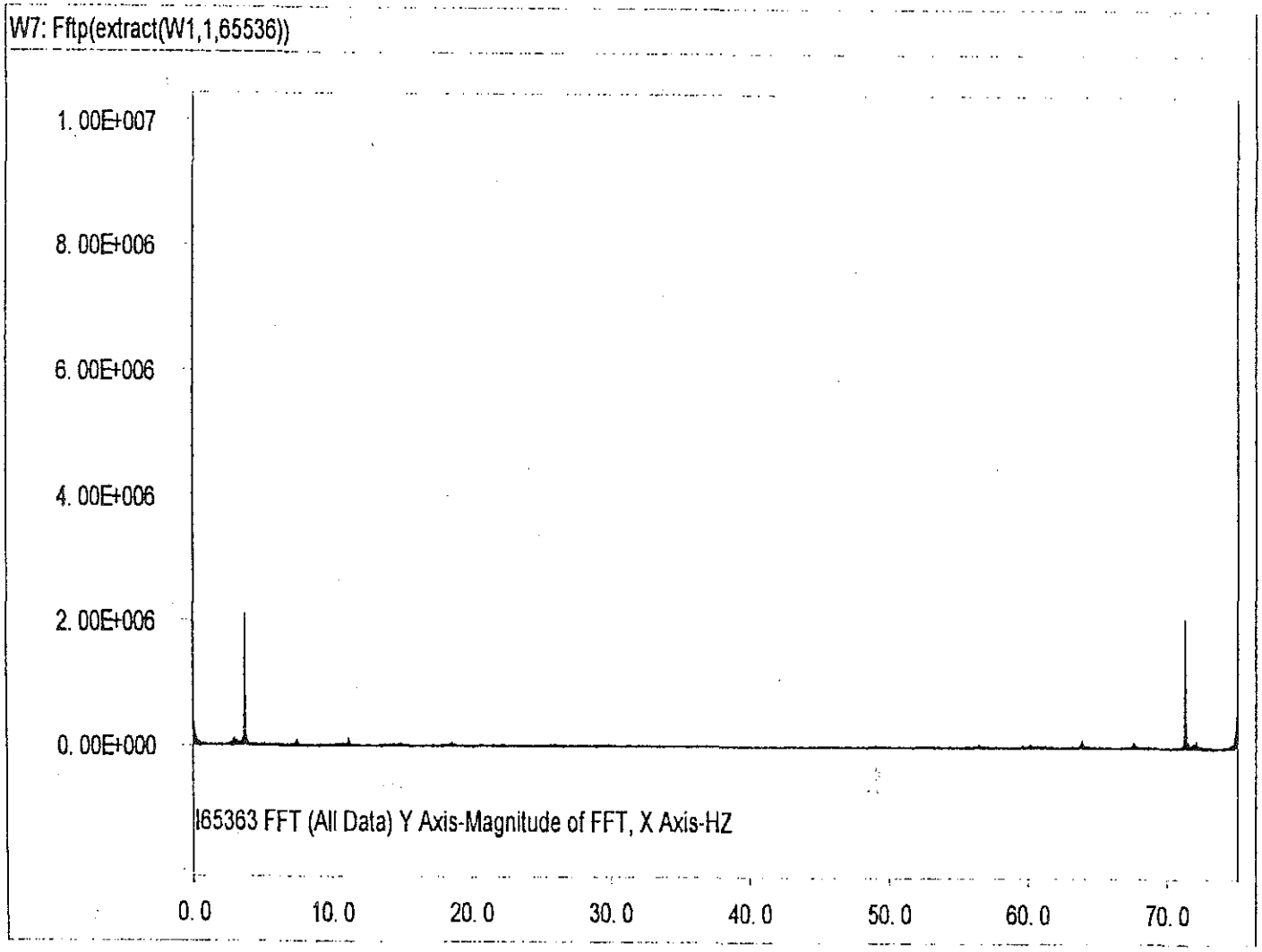

Figure 29. FFT for Live Stress Data from Strain Gage I65363.

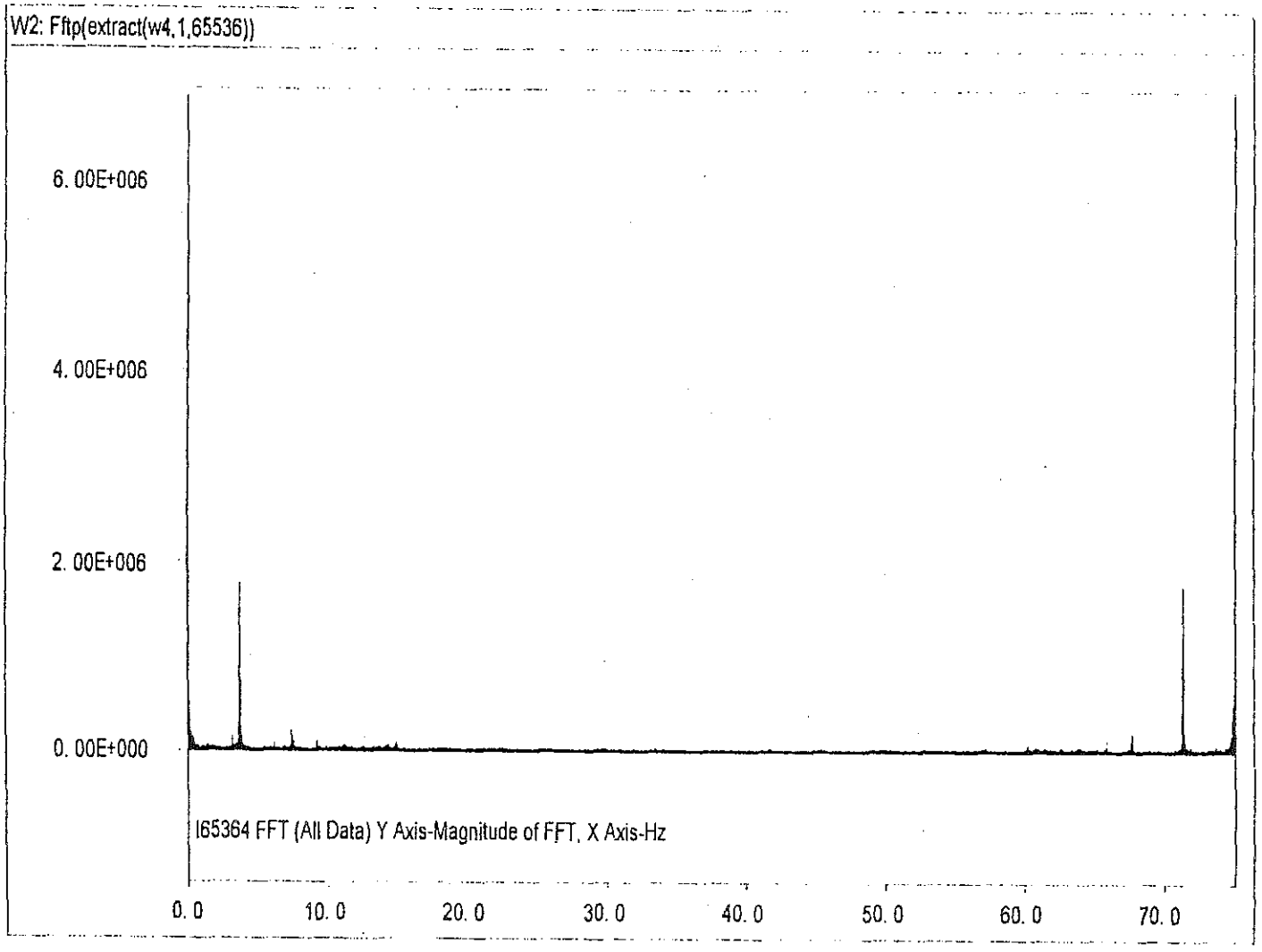

Figure 30. FFT for Live Stress Data from Strain Gage I65364.

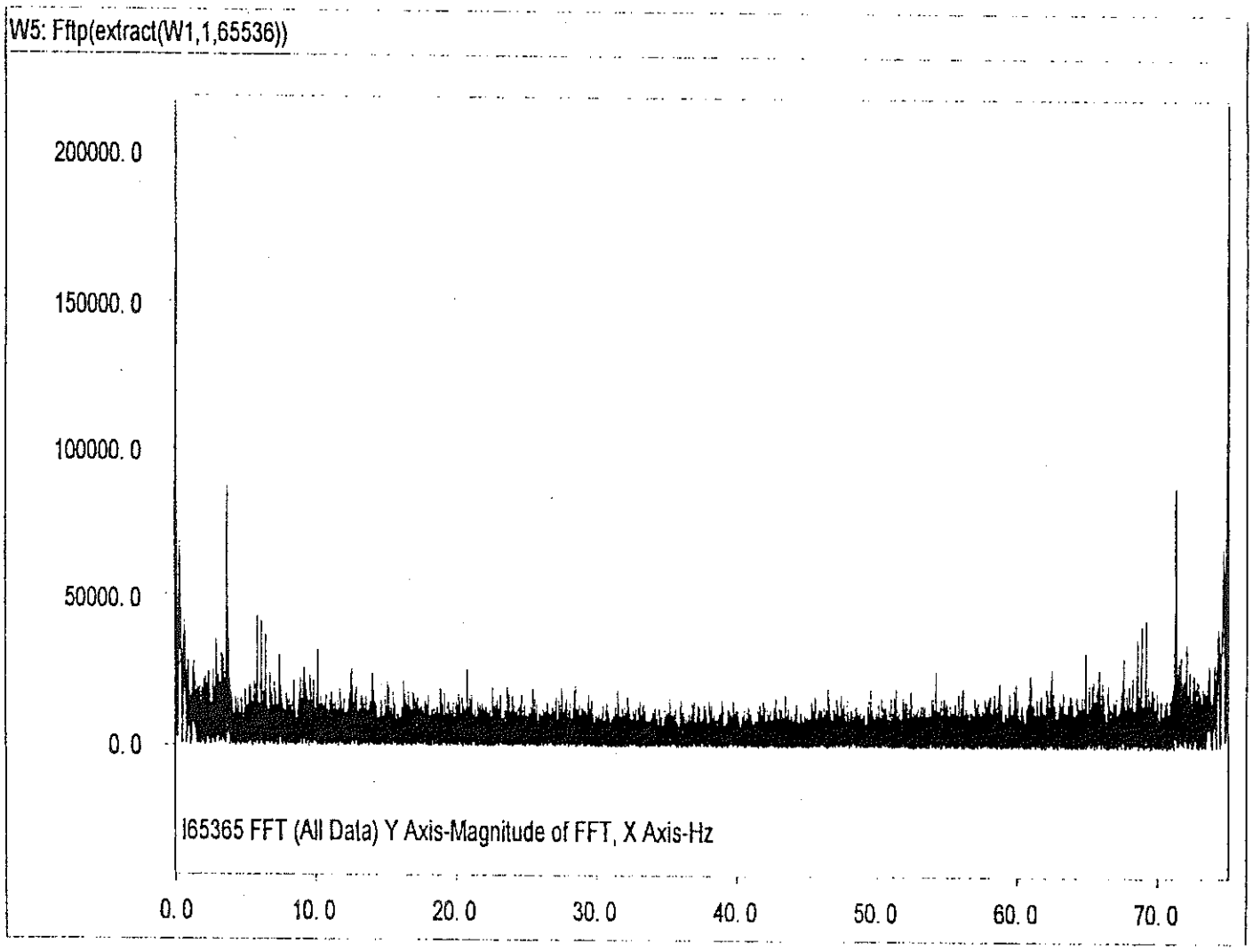

Figure 31. FFT for Live Stress Data from Strain Gage I65365.

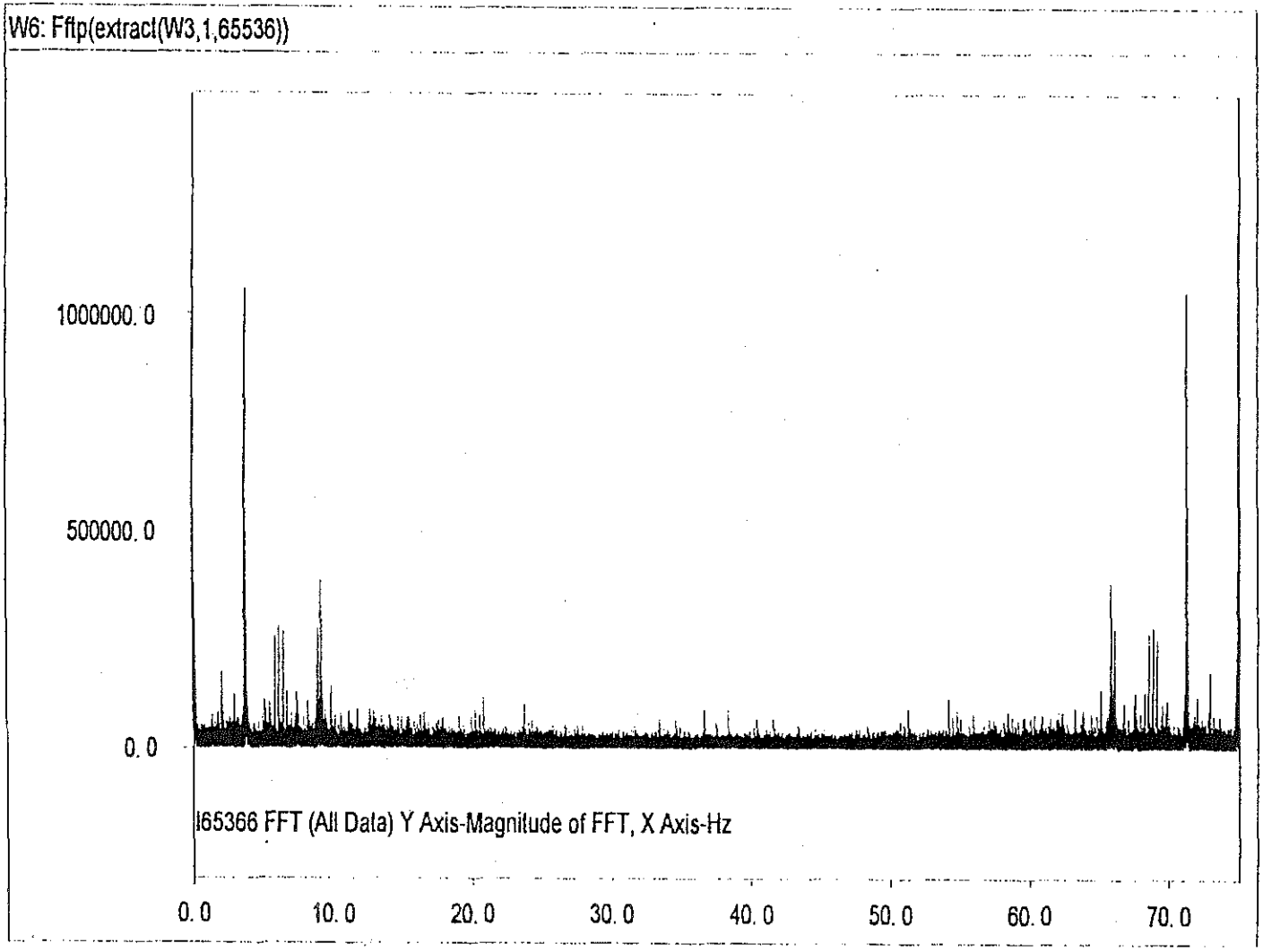

Figure 32. FFT for Live Stress Data from Strain Gage I65366.

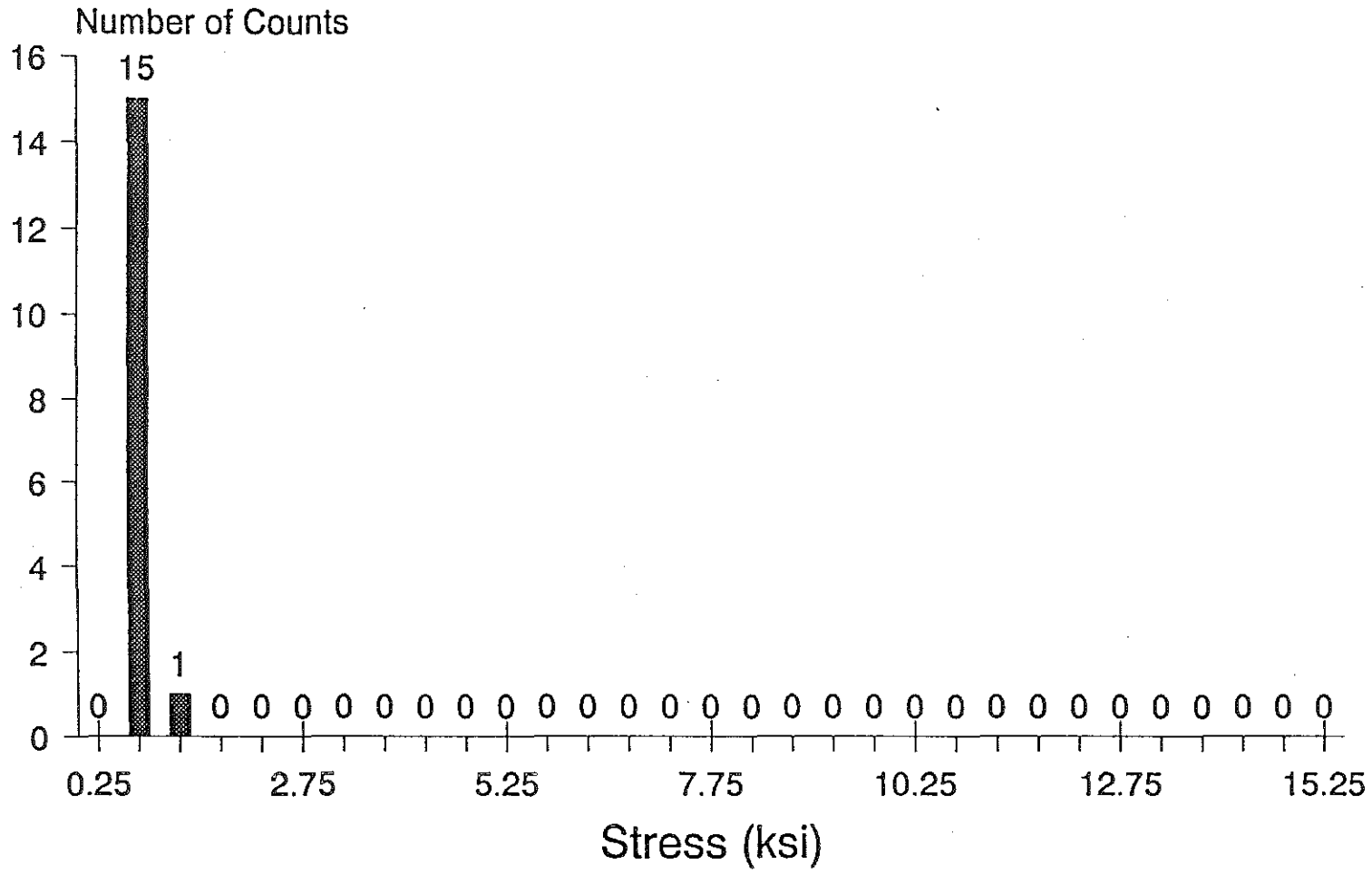

Figure 33. Histogram for Live Stress Data from Strain Gage I6581.

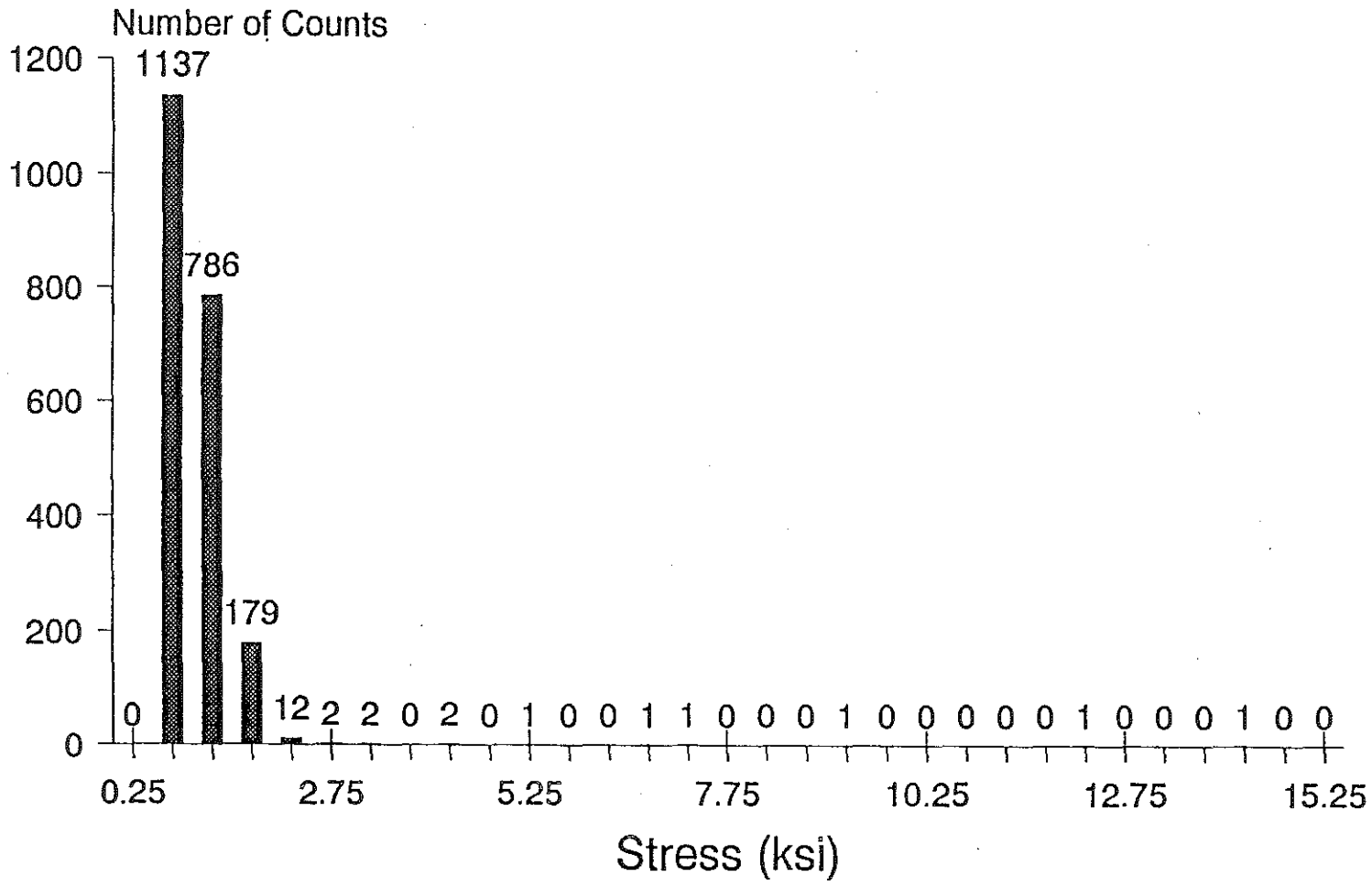

Figure 34. Histogram for Live Stress Data from Strain Gage I6582.

Appendix

(Original Stain Gage Data)

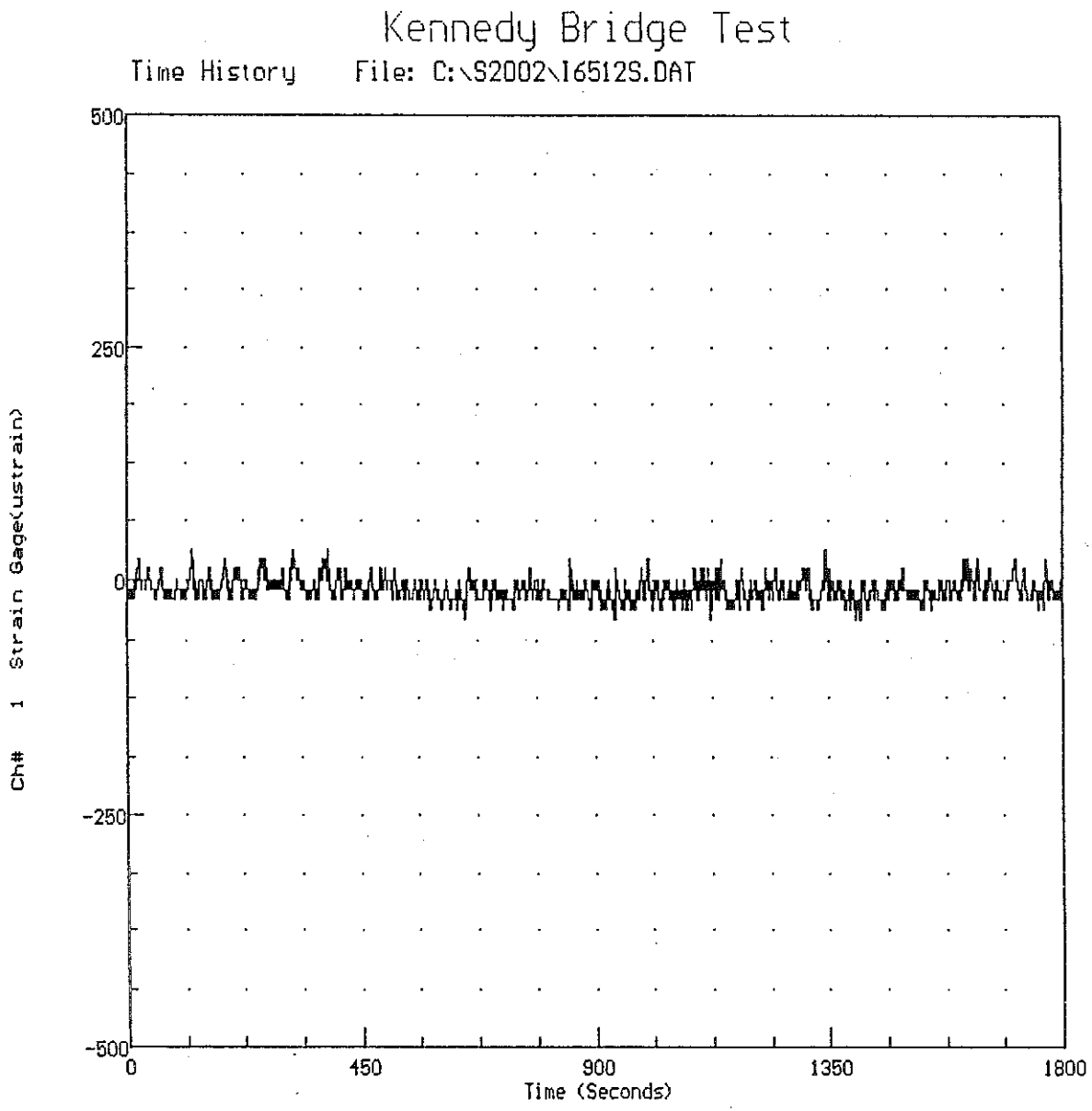

Figure A. Original Strain Data for Strain Gage I65121.

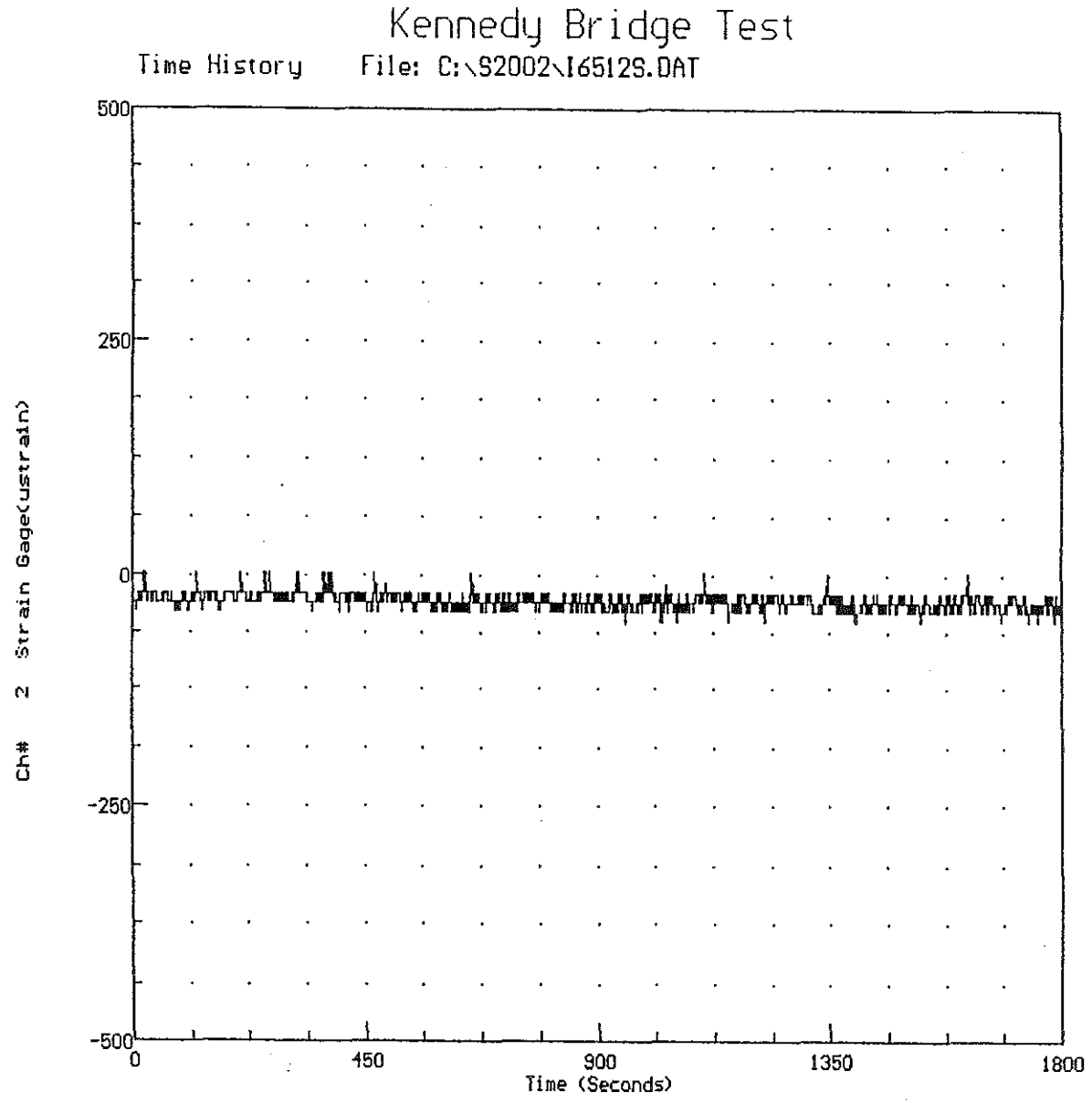

Figure B. Original Strain Data for Strain Gage I65122.

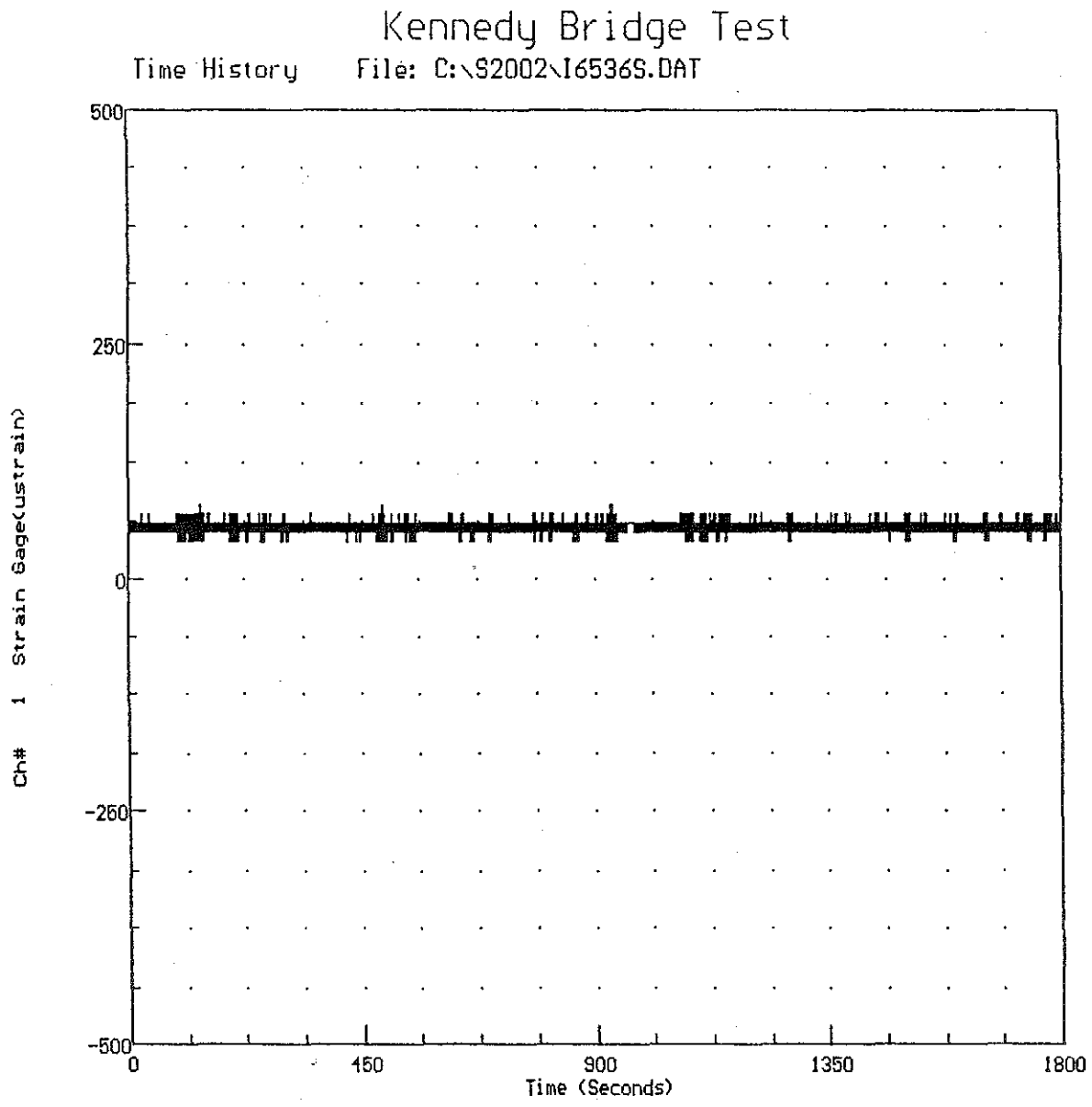

Figure C. Original Strain Data for Strain Gage I65363.

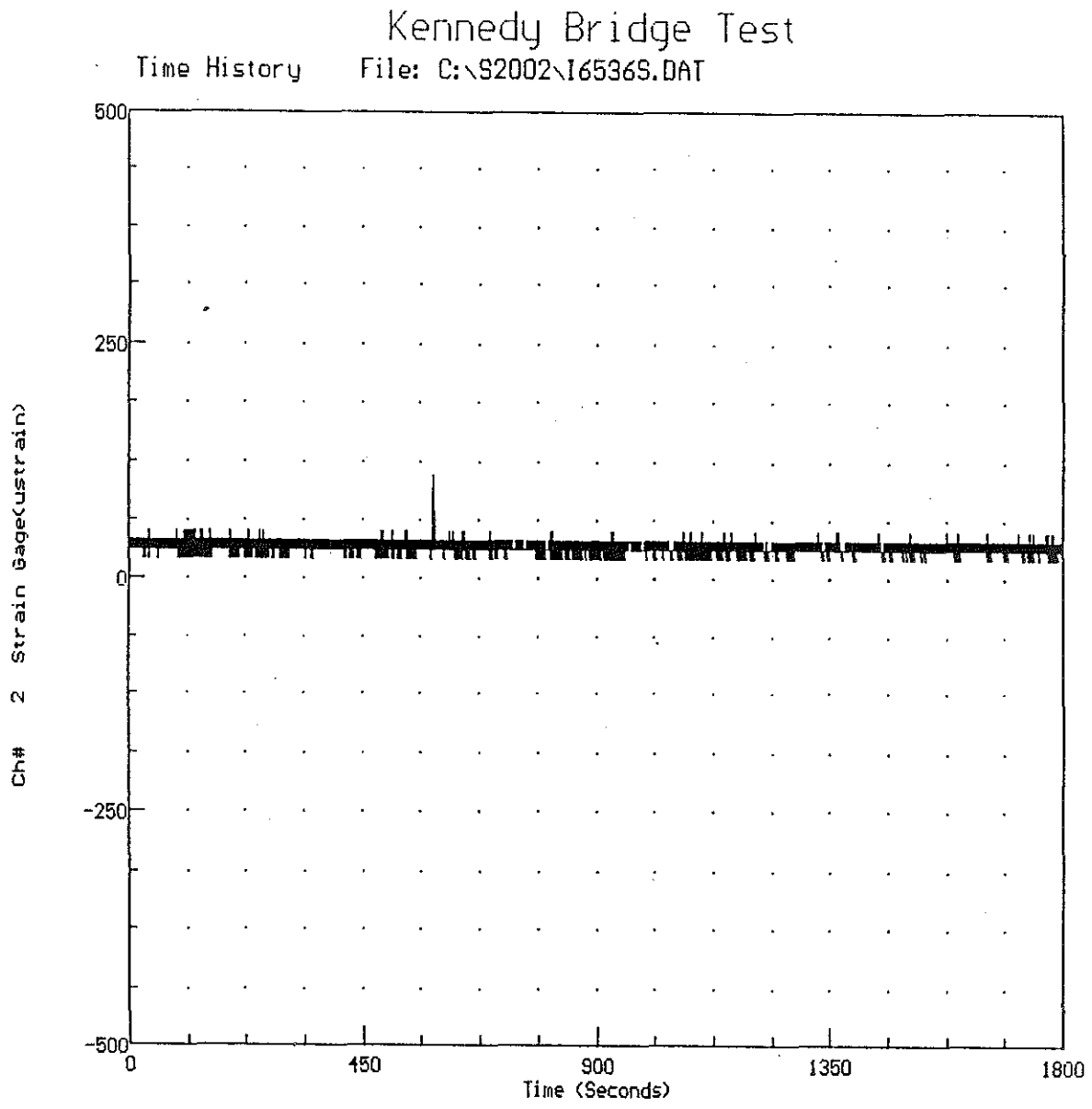

Figure D. Original Strain Data for Strain Gage I65364.

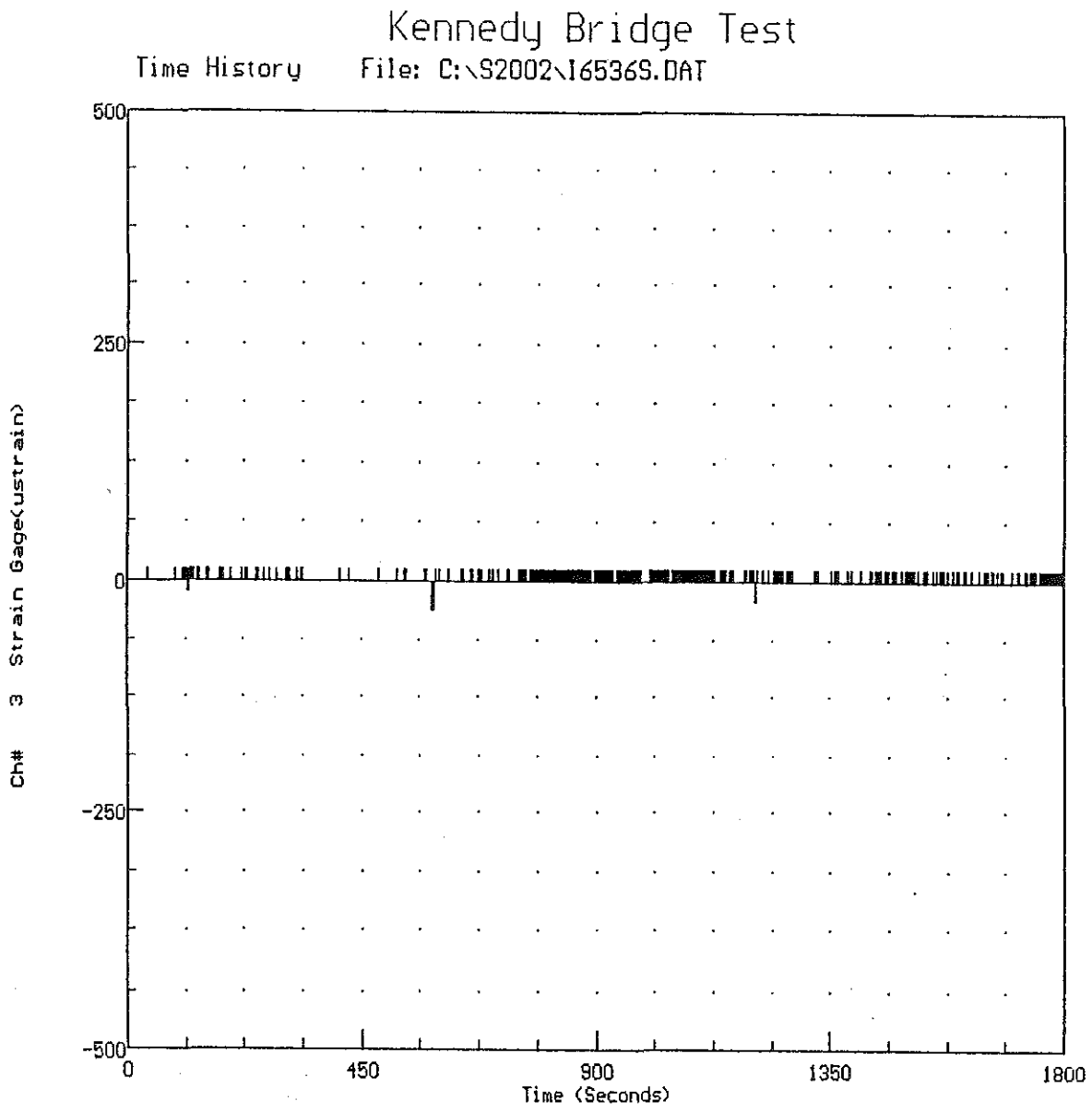

Figure E. Original Strain Data for Strain Gage I65365.

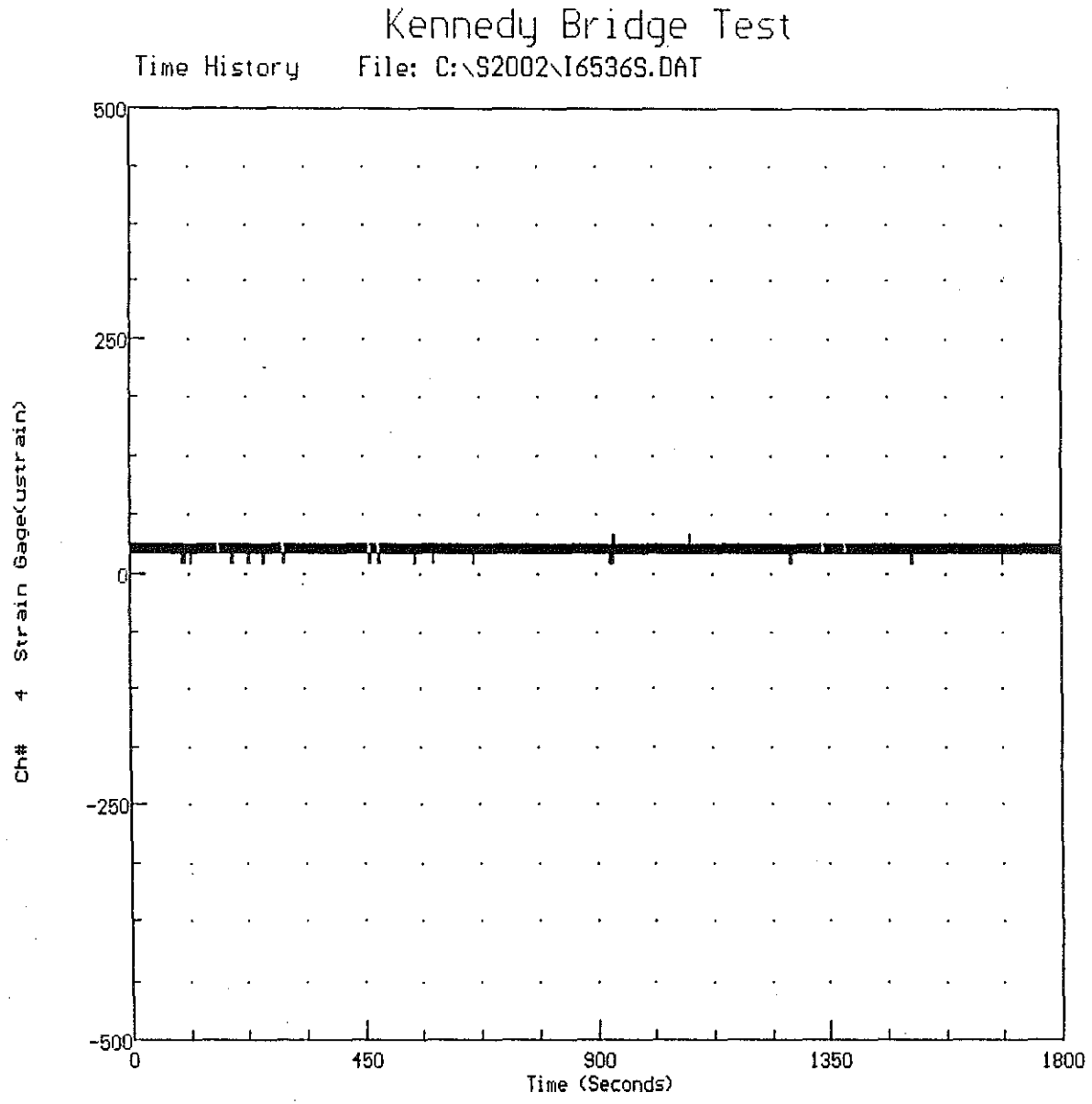

Figure F. Original Strain Data for Strain Gage I65366.

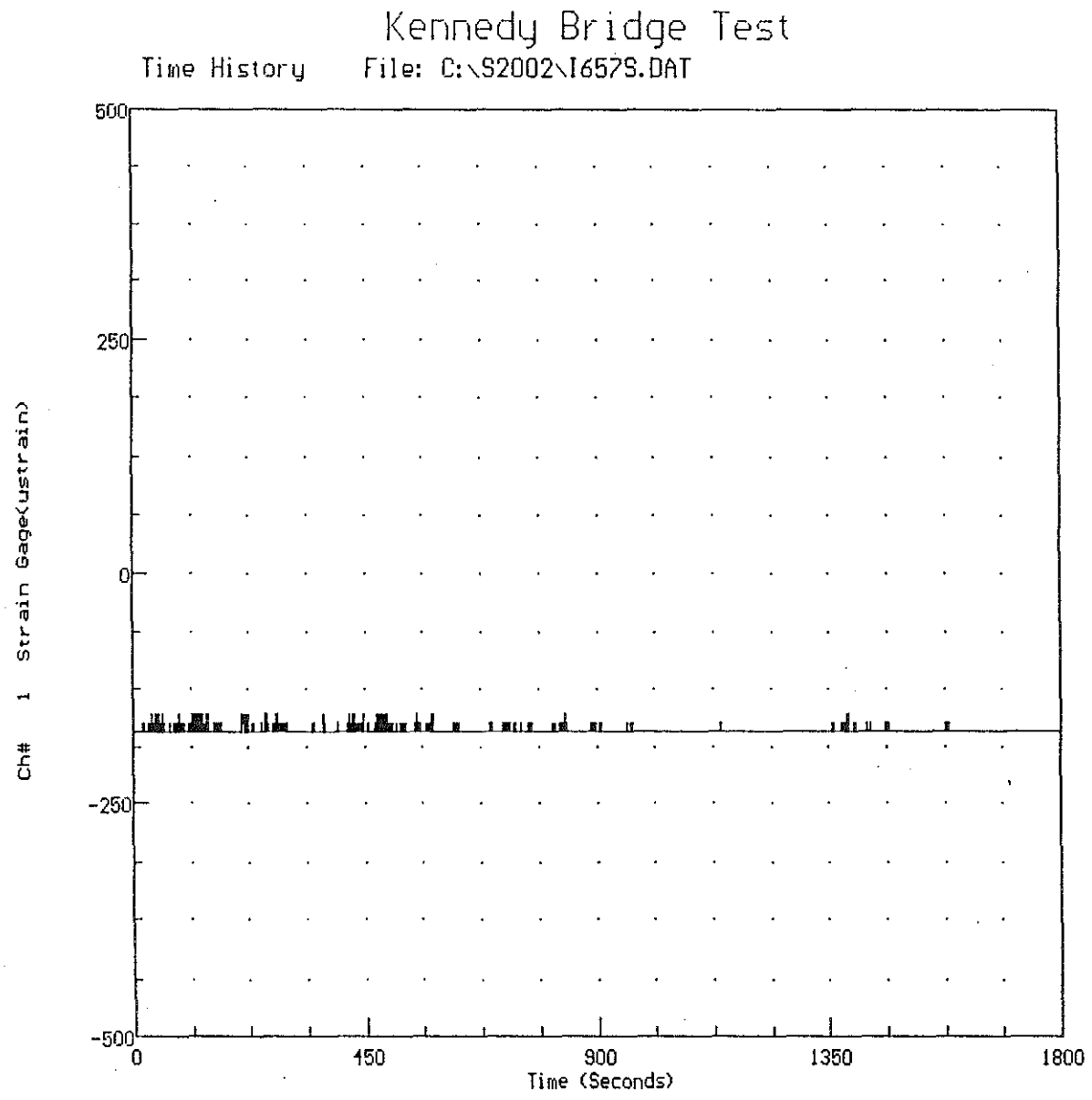

Figure G. Original Strain Data for Strain Gage I6571.

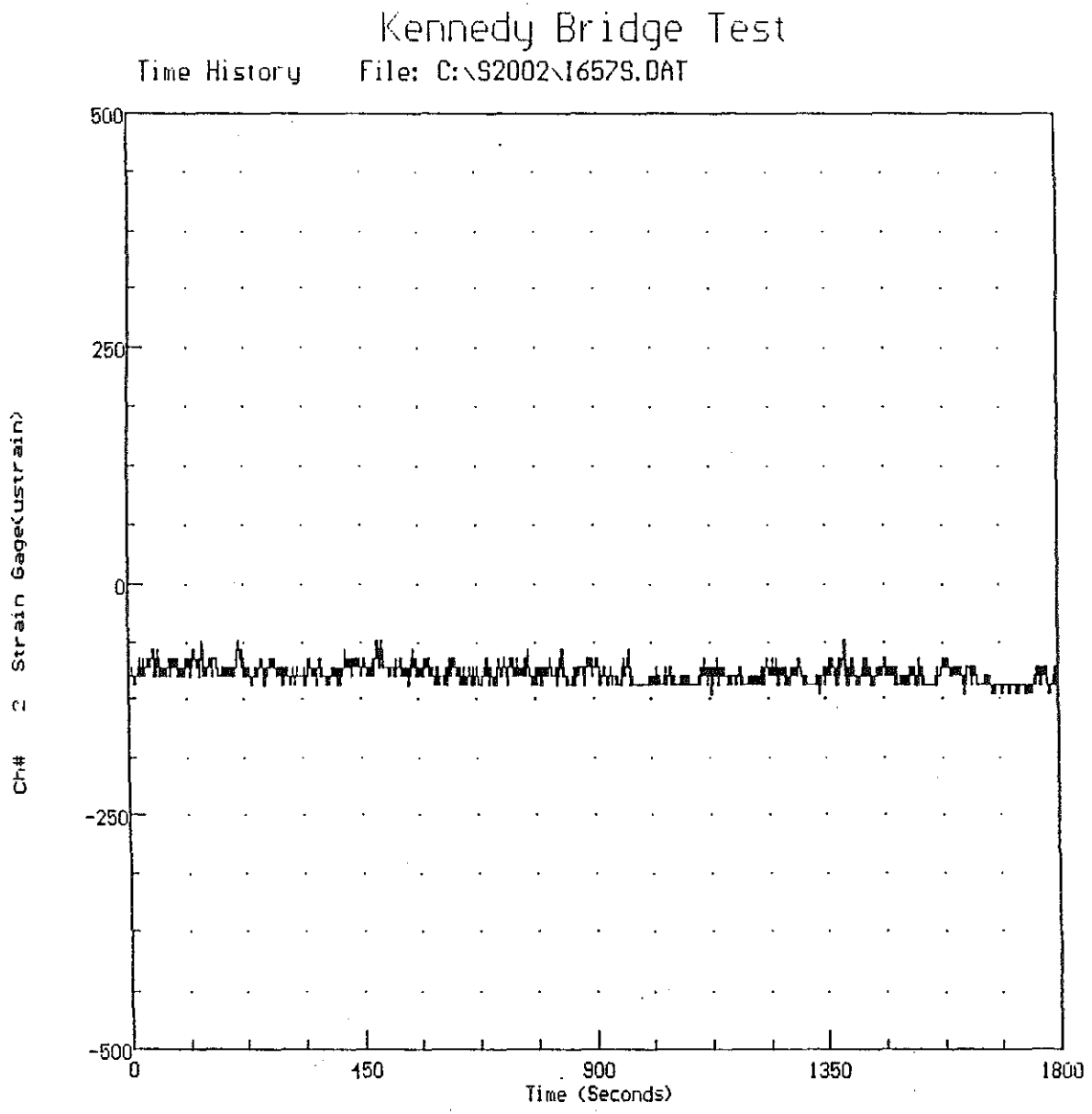

Figure H. Original Strain Data for Strain Gage I6572.

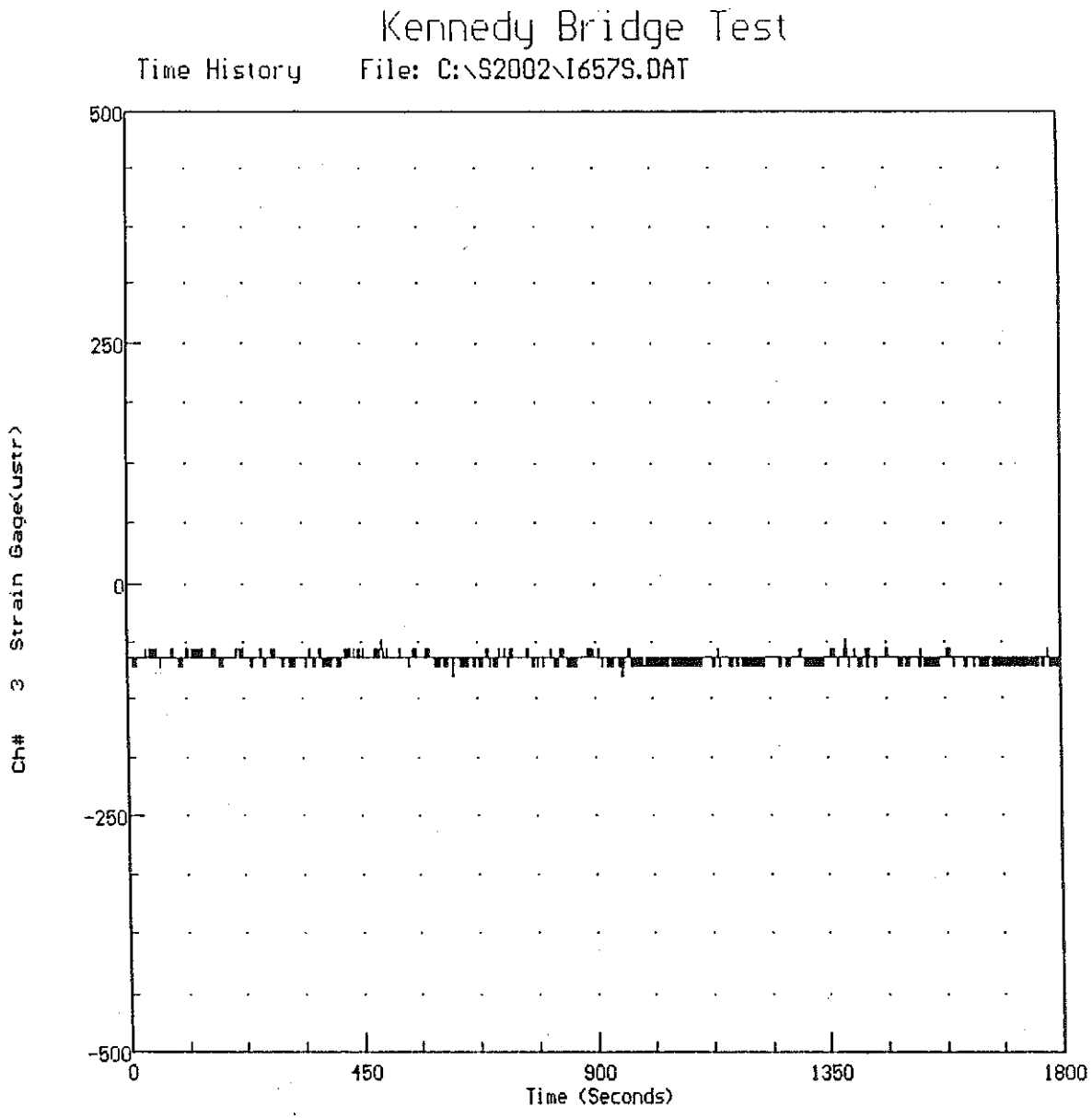

Figure I. Original Strain Data for Strain Gage I6573.